SAPIENZA
UNIVERSITÀ DI ROMA

Decision making driven by mental schemas: study of neuronal correlates of a transitive inference task in dorsal prefrontal and premotor cortex of primates

PhD program in Behavioral Neuroscience
Curriculum: Behavioral Neurophysiology

Dottorato di Ricerca in Neuroscienze Comportamentali – XXXIV Ciclo

Candidate

Surabhi Ramawat
ID number: 1864550

Thesis Advisor

Prof. Emiliano Brunamonti

January 2022

Acknowledgements

I am grateful to all those who have contributed to making this thesis possible. I would first like to thank my supervisor **Prof. Emiliano Brunamonti**, whose constant support and guidance have been invaluable throughout my doctoral journey. His research expertise and scientific approach have helped shape this thesis for the better. I have thoroughly enjoyed my academic pursuits under his tutelage.

I would certainly be remiss to not mention and sincerely thank **Prof. Stefano Ferraina** for his insightful feedback and meticulous scrutiny which helped foster my research project. Additionally, I would like to thank **Prof. Aldo Genovesio** and **Prof. Pierpaolo Pani** for their timely advices and suggestions throughout my doctoral tenure. I thank profusely all my colleagues for being so supportive and helpful at every stage of my research. A big thanks to **Danilo**, **Valeria**, **Stefano** (**Sacchetti** and **Colangeli**), **Lorenzo** (**Fiori** and **Ferrucci**), **Fabio**, **Fabrizio**, **Marta**, **Giampiero**, **Isabel** and **Roberto**, and last but not least, **Francesco**, for always being there to help me out. Special thanks to **Valentina**, **Fabio** and **Giampiero**, who have provided their productive feedback while contributing to this thesis. A debt of gratitude is also owed to my dear friend **Sankalp Tikoo**, for his unconditional support throughout this journey. Lastly, my deepest appreciation belongs to my family and especially to my mother **Dr. Madhulika** for always believing in my potential and motivating me to strive for the better.

Thank you!

Contents

Preface

Brain is a complex network of billions of interconnected cells called neurons, communicating with each other sending electrochemical signals unceasingly. It is incomprehensible how each action or thought, voluntary or involuntary, can be traced back as the aftermath of millions of these electrochemical signals sent and received in specific groups of neurons in a few milliseconds.

Hundreds of years of neuroscience research has led us to where we are today, some mysteries unraveled and some still inexplicable. One of them is the relationship between mind and brain. How are mental processes being translated to the firing activity of neurons? How do different brain areas partake in processing an idea, thought, or action?

Out of the many facets of the mind-brain relationships, in this thesis, we will explore the neuronal correlates of a very specific cognitive process called *Transitive Inference.* Humans and many other animals have been shown to exhibit a capability of making a decision not just based on information acquired through direct experiences but also through linking the previously acquired knowledge and making a decision about something not experienced before. A classic example of such decision-making can be found in the question: if John is older than Mary, and Mary is older than Jack, then who is elder, John or Jack? The answer to this question relies on the inferential capabilities requiring the person to retrieve the relationships learned beforehand, recombine and reorganize them to deduce a novel relationship whose knowledge had not been acquired directly. This ability to deduce is hypothesized to be achieved through the mechanism of flexibly manipulating the previously acquired information to make a decision, termed as *inferential or relational reasoning*.

To this end, we analyzed the single-cell activity recorded from macaque prefrontal and premotor cortices while they performed a Transitive inference task. The prefrontal cortex is a mosaic of psychological faculties, one of the frontal areas responsible for cognitive control and executive functions. On the other hand, the premotor cortex is considered a control center for motor execution and preparation, likely transforming abstract plans in more concrete motor outputs. Interestingly, recent findings point to its role in more complex cognitive processes. The organization of this thesis is as follows.

The *Introduction* presents an overview of Transitive Inference as an aspect of deductive reasoning, the experimental models to test it, various theories devised to support the underlying cognitive mechanisms. In particular, we will consider how decision making in this task is supported by referring to an organized mental schema. Furthermore, we briefly discuss the roles of prefrontal and premotor cortices in this kind of reasoning problem.

Study1 investigates “Different Contribution of the Monkey Prefrontal and Premotor Dorsal Cortex in Decision Making during a Transitive Inference task”, where we explored the neuronal correlates of

these two areas during the manipulation of the supposed mental schema. Here we present a comparison of the roles these areas partake in target selectivity as an aspect of decision making in the transitive inference task. *The findings from this study have been accepted to be published in Neuroscience*.

Study 2 presents the contribution of the dorsolateral prefrontal cortex to the learning and acquisition of the mental schema during a transitive inference task. In this study, we take a step back to study how the prefrontal activity encodes the acquired information from the learning to the test, hypothesized to support the building of the mental schema to be manipulated for taking decisions. The aim of this section is conceptualized as "Neuronal encoding of ranked items in primate prefrontal cortex during different phases of a transitive inference task".

Lastly, the *Conclusion* summarizes all the findings while pointing out some shortcomings, and a few future directions for the results presented in this work.

Introduction

1.1 Transitive Inference

1.1.1 Transitive Inference: an aspect of deductive reasoning

The quest to explore how the brain functions during complex cognitive processes such as problem-solving has led to several experimental paradigms (Funahashi, 2001; Gold and Shadlen, 2007; Jensen, 2017; Zeithamova et al., 2019). Problem-solving based on deductive reasoning by highly intelligent species being one of them.

Transitive Inference (TI) is one such problem, which has been considered one of the aspects of logical deductive reasoning (Vasconcelos, 2008; Lazareva et al., 2020). The following example can give a simple illustration of TI: "Meg is older than Jo and Jo is older than Amy". Then the question, who is older between Meg and Amy can be quickly answered based on the preliminary relational information presented before. Although the information to answer this question wasn't presented directly, it can be deduced indirectly using the information's partial overlapping (relationship of Meg and Amy to Jo). This problem exemplifies a simple task that can be solved using TI, and the fact that humans are readily able to deduce this information is evidence of the TI abilities exhibited by them. TI can be described as a form of reasoning in which, given the preliminary information (the premises), the subject deduces a logical conclusion.

An anthropological perspective regards TI as a hallmark of reasoning based on logical deduction in humans. In modern psychology, this task was first introduced by (Burt, 1911, 2011) in the early 19th century to evaluate the reasoning abilities of children. In 1928, swiss psychologist Jean Piaget explored the basic cognitive abilities of children using syllogisms as illustrated above. The various studies conducted by him (Piaget, 1930, 1955, 1970) have presumably precluded the children younger than around seven years of age from being able to form transitive inferences correctly. These studies theorize that only after the acquisition of logic is the child able to solve problems involving syllogistic reasoning.

However, in 1971, a critically important study (Bryant and Trabasso, 1971) contradicted Piaget's view by illustrating the inability to solve TI problems by younger children was attributed to the memory deficits rather than the deficits of logic. They stated, *"Contrary to the conclusions of Piaget, young children can make transitive inferences if precautions are taken to prevent deficits of memory from being confused with inferential deficits,"* which proved to be one of the seminal findings in developmental psychology.

This study found that four years old children are capable of making correct TI-based decisions during a semi-verbal instantiation of the TI task, given that they have clearly learned and memorized the premises. Hereafter, TI was started to be considered as a general ability to reason and to correctly manipulate the premises according to the rules of logic. The ability of humans to solve the syllogistic problems prior to the development of cognitive abilities pointed towards strong evidence of a simpler mechanism involved in TI than the ones acknowledged before. As a result, more studies have emphasized the mental model approach in relation to the TI task (Johnson et al., 1996; Acuna et al., 2002b; Merritt and Terrace, 2011; Jensen et al., 2021).

These new findings consequently paved the way to the scientific question, which was incongruous previously, "*Are non-human animals correctly able to solve TI tasks?"* This question was first addressed by McGonigle and Chalmers in 1971, where they were able to successfully demonstrate a TI task with squirrel monkeys. Consequently, many others have followed and studied the TI processes in rats (Dusek and Eichenbaum, 1997; Van Elzakker et al., 2003), chimpanzees (Gillan et al., 1981; Boysen et al., 1993), monkeys (Treichler and Van Tilburg, 1996; Brunamonti et al., 2014, 2016), pigeons (Weaver et al., 1997; Wynne, 1997), pinyon jays (Paz-y-Miño C et al., 2004), hooded crows (Lazareva et al., 2004) and fish (Grosenick et al., 2007) and chicks (Daisley et al., 2021).

These studies are landmarks for establishing cognitive and neuronal models in non-human animals for understanding complex mechanisms involved in deductive reasoning in this form of decision-making. In many of the species these abilities are directly linked to the social hierarchy formation.

1.1.2 The transitive inference task

Experiments on Transitive inference have employed different versions of the TI task to study the behavioral and neuronal basis of deductive reasoning in humans and animals. However, most research aimed at studying TI in non-human animals is based on the n-term series task. This form of TI task design was originally developed for children (Bryant and Trabasso, 1971) and later modified to be implemented with non-human animals (McGonigle and Chalmers, 1977) into a non-verbal version. The simplest form of this task involves five different stimuli, and Figure 1.1 shows the example of stimuli pairs presented during the training and the test.

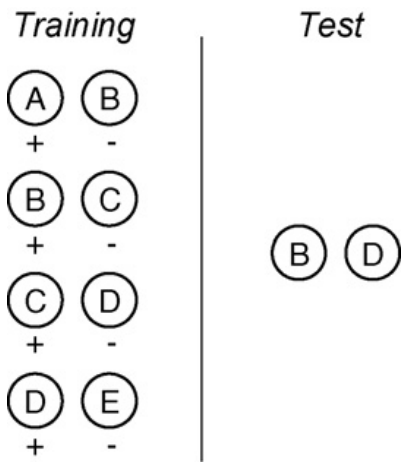

Figure 1.1. Illustration of an n-item series TI task schematic (n=5). Each letter represents a unique stimulus, paired with another stimulus to be presented simultaneously during training (left panel) and the test (right panel). The + and – sign in each of the presented pairs indicates the reinforced and the non-reinforced choice respectively in that particular pair. (*adapted from Vasconcelos, 2008*)

In Figure 1.1, each pair represents the simultaneous comparisons of the stimuli, with the ones indicated with a "+" under them are being reinforced while the ones indicated with "– "sign are non-reinforced. Each letter in the task design represents a unique stimulus associated with it. Depending on the experimental model and species involved in the experiment, the stimuli are chosen to be visual or olfactory. The schematic of n-series items here shows a 5 item series task, with the overlapped information presented with the pairs comprising B, C and D; e.g., when presented with A, B is not reinforced, but with C, it is. The presentation of pairs within the training set seemingly creates a linear rank-ordered series represented as A>B>C>D>E. The pair B vs D accounts for a critical pair during the test, as these two items were never presented together during the training, and they were partially reinforced. The reinforcement history of both of them was 50%, i.e., they were reinforced during half of the presentations in training. The correct choice, i.e., stimulus B during the test phase, suggests that the subject could deduce the relationship using the TI strategy. One of the most critical aspects for testing TI using an n-series is the value of *n*, which cannot be less than 5, as the contemplated test pairs in an item series consisting of less than five items would always include an end-anchor item of the series, making it the choice discrimination uninformative of inferential reasoning.

The training for this simplistic task design has been reported to be implemented using two strategies: Sequential and Intermixed designs (Vasconcelos, 2008). *Sequential* training is described by the procedure of training on one discrimination by itself until the performance criterion of 90% or above is achieved, and then the subsequent discrimination in the sequence is trained using the same criterion until all the discriminations are learned (Weaver et al., 1997; Benard and Giurfa, 2004). On the contrary, the *Intermixed* design follows the presentation of all the discriminations concurrently in an arbitrary

order, making the training time considerably longer (McGonigle and Chalmers, 1977; Boysen et al., 1993; Wynne, 1997; Van Elzakker et al., 2003; Lazareva and Wasserman, 2006; Brunamonti et al., 2011, 2016). Most studies have implemented the TI task training using intermixed training, with a preceding sequential training block concluded by a training block of concurrent presentation of all the training pairs.

Some exceptions to an n-term series TI task design have been reported in a few studies (Paz-y-Miño C et al., 2004). In this unique study, the task design consisted of the pinyon jays subjected to a social interaction task, where the wild-caught birds were divided into two groups. After establishing the social dominance within the groups, each of the birds from both the groups observed two other birds interact over a peanut, one from its own group and one from the other group. The critical test allowed a social interaction between the observer and a member of the other group, observed previously by the observer, being dominant with the dominant member of its group. This experimental design tested the hypothesis if this highly social species can infer the social status using the strategy of transitivity by exhibiting a submissive behavior when tested for the critical social interaction. This study demonstrated that pinyon jays used TI in social settings and such cognitive capabilities are prevalent in a large number of social species. This task design can account for TI in social dominance in many species, except the ones where physical features can infer dominance.

1.1.3 Transitive inference task: performance considerations

As stated previously, one of the procedural restrictions to be considered in using an n-term series task design is the value of *n*, which cannot be chosen to be less than 5. A more extended series of items in the task design (>5) facilitates more number of transitive tests (i.e., the test pairs excluding the anchor items). Another possibility provided by a more extended series is the number of intervening terms in test comparisons, i.e., the terms between the items compared in the test pairs. For example, in a 6-term series task, A>B>C>D>E>F, the number of intervening terms between the transitive test pair B vs D is one (C), while in the pair B vs E, it is two (C and D). Numerous studies in humans and non-human animals have demonstrated that performance accuracies and reaction times are governed by the effect of the number of intervening terms. The difference in the number of intervening terms directly refers to the rank differences between the items of the test pairs and is termed as symbolic distance on the scale of linearly ordered series.

Symbolic Distance Effect: The response accuracy during the test increases, and the reaction time decreases as the number of intervening items (symbolic distance) increases. This phenomenon is termed the Symbolic Distance effect (SDE). Among the numerous studies which have reported the observance of SDE in subject's behavior, however, in some of them, the SDE is considered to be confounded by two primary concerns, the first-item effect and the different number of data points for each symbolic distance (Von Fersen et al., 1991; Wynne, 1997). Figure 1.2 shows the schematic of a test session after the training for a TI task using a seven-term series task. The first item effect refers to the observation

of higher performance accuracy for the pairs belonging to the same symbolic distance but closer to the always-reinforced end-anchor of the series. This confound can be taken care of by considering the mean accuracies across all the symbolic distances. Another concern is unequal data points for different symbolic distances; e.g., the more prolonged the distances would be; the fewer data points would contribute to the average. This problem can be evaded by only studying the SDE within a given distance from the always-reinforced item of the series (e.g., BD vs BE vs BF; Figure 1.2).

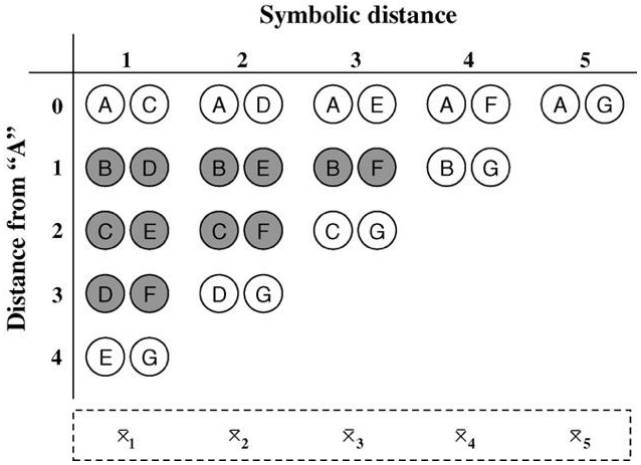

Figure 1.2: Task schematic during the test session of a 7-term series TI task. The Xn on the x-axis represents the symbolic distance, and the pairs shaded in grey are the pairs characterizing true Transitive test pairs (*adapted from Vasconcelos, 2008*).

Another behavioral effect accounting for the behavioral performance during a TI task is how accurately the subject learns the series? However, the ideal case would be to have a comparable, above chance level performance for every premise, but it is not the case most of the time. The performance accuracy follows a 'U-shaped' analogy, where the pairs containing the end anchors are solved with higher accuracy than the interior ones.

Serial Position effect: This effect is exhibited as a typical retention function obtained in the immediate serial recalls is referred to as the serial position effect (Figure 1.3; (Bryant and Trabasso, 1971; Woocher et al., 1978).

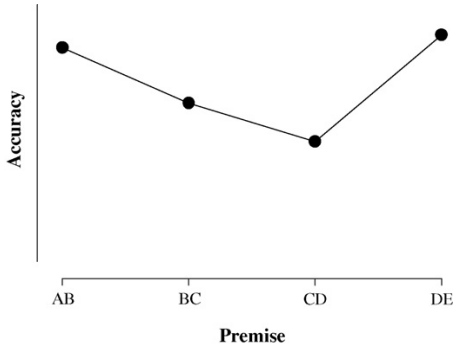

Figure 1.3: Serial Position curve. U-shaped performance curve during the training of adjacent pairs of a 5-term series TI task (*adapted from Vasconcelos, 2008*).

Together SDE and SPE have been suggested to be the evidence of integration of list items learned by humans and monkeys to form a linear representation of the list items (D'Amato and Colombo, 1990; Treichler and Van Tilburg, 1996; Merritt and Terrace, 2011; Brunamonti et al., 2016).

1.1.4 Transitive inference models

Among several lines of research proposing the plausible mental mechanisms involved in solving the TI task, some are based on cognitive models like the mental representations of the series items or the mental line. At the same time, most consider the models which are behaviorally explainable, like the reinforcement history and the relative frequency of the item occurrences.

Cognitive models accredit the phenomenon of TI to problem-solving based on formal logic or the use of a mental model. In the context of human studies, this ability is ascribed to the arrangement of information as mental models or logic to solve these problems. According to Piaget's view in the 19th century, transitive syllogisms are solved by coordinating the information acquired during the premise learning and logical rules based on the language. As stated in the previous section, Piaget's was based on the idea that the children who had not reached the concrete operational stage (old enough to apprehend and use the rules of logic fully) were incapable of TI. However, this view was questioned, and the view on the logical mechanism to solve everyday problems involving TI changed in the following years. In humans, the possibility of the decisions based on an arrangement of information in the form of a mental model was instead proposed and studied (Trabasso and Riley, 1975; McGonigle and Chalmers, 1977; Sternberg, 1980; Acuna et al., 2002b). In particular, these studies have focussed on spatial paralogical models instead of relying on logical principles. This paralogical model assumes that the acquired knowledge on the premises learned independently during an n-term series task training and is integrated by the subject to form a series of mental representations or a spatial schema of information. When the subject is required to solve a TI problem, a decision is supported by the information that how far is the items in the presented test pairs located from the series end items on this spatial representation of the information. Hence, a correct TI decision is based on accessing this mental representation rather than using a formal logical deduction.

The theories of spatial representation of premise information have also been accounted as a fundamental cognitive model in non-human animals. It is proposed that the animals integrate the premises to form an ordered series while solving a TI task. Most studies based on postulating this theory have reported the premise information to be integrated as a symbolic spatial representation. However, different studies have reported this integration at what stage this integration occurs. For instance, a model proposed by the study (Bryant and Trabasso, 1971) supports the idea that the subject forms independent representations of the premise pairs during the training, and these representations are integrated into a mental line only during the test phase. Contrarily, most spatial paralogical models favor the theory of the integration of information directly during the training (e.g. De Soto et al., 1965)

Aside from these theories, the fundamental questions still persist. *How is this mental schema constructed?* Moreover, *how are these spatial representations lead to the signature performance effect?* One explanation for these models is that the end anchor items of the series (always-reinforced or non-reinforced) are located at the ends of the supposed mental line before all the other items. The other acquired premises (stimuli) are then ordered between these end-anchors as the training progresses. Once this line is formed, it is used to solve any discrimination during training or testing via a spatial search along the imaginary line. In addition to this, the way the mental line is constructed, i.e., inwardly, explains the SDE and SPE.

The SDE is explained by the positions of representations of the stimuli in the series. The closer the stimuli would be in the series, the more similarity would be observed in the spatial representations, giving rise to more difficulty in discriminating the items. At the same time, the SPE is accounted for by the unambiguous nature of the end anchor items. Since the pairs including these items do not have an ambiguity of reinforcement, the accuracy of choosing the correct item is higher, while the pairs with non-end anchors have an ambiguous reinforcement history, resulting in a greater difficulty in making the correct choice.

However, this argument explains the translation of the performance signatures from the mental representation; it does not accommodate the possibility of a sequential training, where the end anchors are cannot be placed first on the mental lines, and the last item of the series is presented at last. This type of training clearly violates the end-inward construction of the mental line, suggesting the integration of information during the test after acquiring individual premises during the training.

1.2 Neuronal basis of Transitive Inference

Many studies have explored the brain mechanisms and circuits underlying deductive reasoning and, in particular, the neural substrates of transitive inference. A transitive inference task is essentially a decision-making task. The choice decision relies on integrating past experiences characterized by overlapping features and using that learned information to make decisions about those indirectly related experiences. It represents the form of reasoning that humans and other species solve by internally manipulating spatially organized information rather than relying on formal logic for deducing the correct decision of the problem.

Several human neuroimaging studies have identified the cortical regions activated during the experimental paradigms related to reasoning and internal knowledge formation. This domain of neuroimaging studies has employed various task designs to study neural processes underlying TI. For instance, (Acuna et al., 2002a) used a non-verbal 11-item ordered list TI task to train human subjects, and they found activations in bilateral PFC, pre-supplementary motor areas, insula, precuneus, and lateral posterior parietal cortex. Another study by (Heckers et al., 2004) found task-related activations in the bilateral frontal-parietal-temporal system, including the hippocampal cortical circuit. Other neuroimaging studies employing human paradigms using explicit verbal inference, like '*George is*

taller than Mike; Mike is taller than Lynn; George is taller than Lynn' have reported the activations in bilateral parietal-frontal and bilateral temporal systems (Goel and Dolan, 2001; Knauff et al., 2003). A paradigm involving the transitive inferences based on the knowledge of *previously learned information like familiar geographical locations* invoked activation in the bilateral hippocampus, in addition to activations in parietal-frontal systems (Goel, 2004, 2007). These studies suggest that this aspect of reasoning involves large brain circuits functionally connected in a complex network. Figure 1.4a shows the overall network of the activated brain areas during a TI task (Goel and Dolan, 2001). Based on the content and context of the presented stimuli, these human neuroimaging studies suggest that the left-lateralized frontal-temporal system processes familiar or conceptually coherent contexts of reasoning (Figure 1.4b), e.g., all apples are red, red fruits are nutritious; hence all the apples are nutritious. On the other hand, the processing of an unfamiliar or non-conceptual set of information, e.g., arbitrarily selected stimuli linked to a set of rules, A>B and B>C, hence A>C leads to activation of bilateral parietal visuospatial systems consisting of bilateral parietal lobes and dorsal PFC (Figure 1.4c; (Goel et al., 2000).

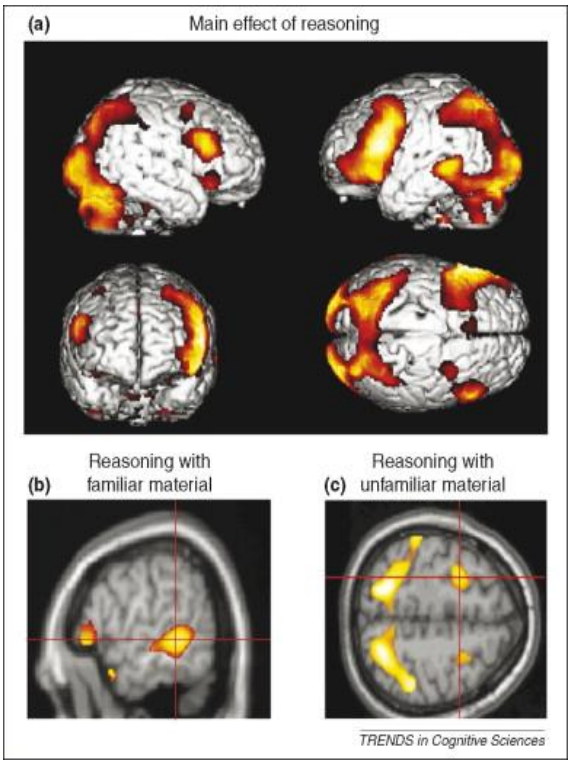

Figure 1.4 Network of activated brain regions during a transitive reasoning task in humans, a. The main effect of reasoning observed in the bilateral network including the occipital, temporal, parietal and frontal lobes and basal ganglia. **b.** Reasoning about a familiar context or conceptual information activates the left frontal temporal system. **c.** Bilateral activations parietal lobes and dorsal PFC during the reasoning task performed with a set of unfamiliar or non-contextual information. (*adapted from Goel 2007*).

Apart from these neuroimaging studies, the neurophysiological research in animal models has provided with the knowledge of cortical and hippocampal areas participating in the information accumulation and manipulation after retrieval during tasks involving reasoning (Dusek and Eichenbaum, 1997; DeVito et al., 2010; Pan et al., 2014; Falcone et al., 2016; Mione et al., 2020). These studies have highlighted the Prefrontal cortex to be responsible for manipulating the information during deductive reasoning and managing the mental schema by reflecting the behavioral effects of TI task in the single-cell activity in the primate brain (Brunamonti et al., 2016). Likewise, the premotor cortex is reported to encode the task difficulties during the test phase of the TI task with non-human primates during the selection of the target item (Mione et al., 2020). Led by these findings, the following section reviews the role of Prefrontal and Premotor cortices during decision making in the context of deductive reasoning and transitive inference.

1.2.1 Role of prefrontal cortex in deductive reasoning

The prefrontal cortex has been proven to play a crucial role in higher cognitive functions like attention, working memory learning, and manipulating task variables. PFC is an elaborate neocortical area in the primate brain that sends and receives projections from virtually all the cortical sensory and motor systems and other neocortical areas, making it a fundamental cortical region participating in executive control. Damage to PFC has been reported to cause deficits in planning, judgment and decision making (Goldman-Rakic, 1988; Funahashi, 2001). An inability to perform all these functions was considered a decline in executive controls; however, the executive control cannot be explained by one single mental process. It is an umbrella term including adequate planning, judgment, decision making, reasoning, and monitoring external and internal states. Animals and patients with prefrontal lesions have been reported to show normal IQs and long-term memory functions. However, they exhibit a diminished capacity of insight and foresight, poor planning and judgment, and deficits in working memory (Stuss and Benson, 1986; Funahashi, 2001). In the context of deductive reasoning during a transitive inference task, rule formation and episodic memory are some of the most important aspects. Various neurophysiological studies have accounted for the PFC activity during a spatial working memory task, such as the oculomotor delayed-response task has revealed that a large population of PFC neurons exhibit a delay period activity (Watanabe, 1986; Funahashi et al., 1989; Carlson et al., 1997). The neurons from dorsolateral PFC (DLPFC) primarily represent spatial information of visual cues during the delay period as a labeled line code. Different neurons code different spatial locations of the cues while the same neurons keep encoding the same visual cue repeatedly. These findings support the evidence that the DLPFC participates in episodic or working memory, and also it contains the complete memory map of the visual space, where the cues are presented at different locations (Funahashi et al., 1989). Similar studies using a delayed response task have reported delay period activity in PFC neurons exhibit the positional preference as well as the information regarding the saccade direction (Funahashi, 2001). These results indicate that the PFC neurons encode the task goals and features during a working memory

task (Funahashi, 2001). Considering the involvement of PFC in distinct cognitive mechanisms, the role of PFC in terms of working memory has been postulated as a working memory model (Figure 1.5).

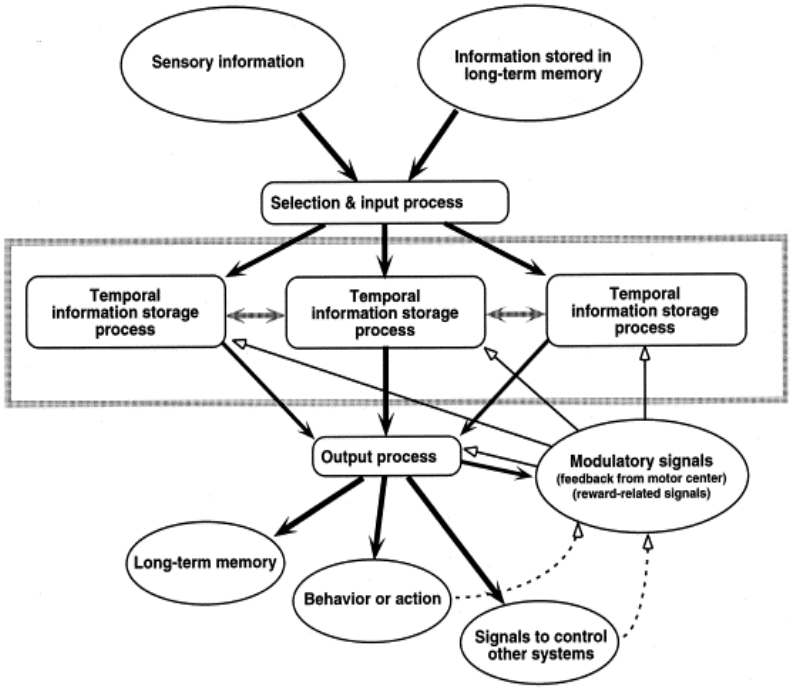

Figure 5: Model explaining the role of PFC working memory processes in executive control. The model emphasizes on the dynamic interactions among different processes and dynamic interactions between storage processes (*adapted from Funahashi 2001*)

In addition to the role in working memory, the PFC has been studied to be involved in associative learning during a conditional visuomotor task. The findings suggest that PFC activity ideally represents the specific cue response conjunctions, signifying that PFC neurons can integrate diverse behaviorally relevant information (Asaad et al., 1998). Visual stimuli can be categorically represented by the lateral PFC (LPFC) neurons. (Freedman, 2001) has shown that the LPFC neurons encode the category information distinctly during a delayed match to a sample task. The stimuli used in their study were created using partially morphed images of two distinct categories blended using different proportions and systematically modified to vary the shape and a defined category boundary. At the same time, the neuronal populations during the sample presentation and the delay periods have been shown to distinguish between the categories but not within the categories (partially morphed images of two categories). Involvement of LPFC in reward prediction during the pair association tasks and manipulation of information during a variation of the delayed match to sample task have also been reported (Pan et al., 2008; La Camera et al., 2018). The DLPFC neuronal activity has also been shown to form associative representations, e.g., associations between pairs of pictures or colors and sounds, which is an indispensable mechanism in relational reasoning. These associative mechanisms in DLPFC were highlighted in the study (Diester and Nieder, 2007), where they showed that the DLPFC neurons signal the meaning of signs. They recorded single-cell activity from the DLPFC and posterior parietal

cortex of macaque monkeys trained to associate the Arabic numerals (symbols) with the numerosity of dot patterns within the range of one to four. The performances of the monkeys while associating the symbols to the numerosity exhibited typical patterns of analog magnitude judgments, such as the numerical distance and size effect.

In addition to all these neurophysiological evidence of involvement of PFC in higher cognitive functions in various contexts, a few studies have studied the direct involvement of PFC in transitive inference. A lesion study (DeVito et al., 2010) reported that damage to the medial prefrontal cortex (mPFC) in mice leads to a delay in learning the series items during a TI task. However, a severe impairment was reported in making the transitive judgments, while the performance of the mice with mPFC damage for the non-transitive probe trials was comparable to the control group. These results indicate an important role of PFC in learning overlapping associations and in deduction-based reasoning. Another study has deeply explored the neuronal modulation in PFC in a TI task (Brunamonti et al., 2016). The authors have reported that the DLPFC activity recorded from the macaque brain while they performed a 6-term series TI task was found to be modulated by the task-related variables like the SDE (symbolic distance effect) and the SPE (serial position effect). They further argue that the activity patterns in DLPFC during the test phase of the task reflect the task's behavioral effects and indicate the manipulation of underlying mental schema constructed during the TI task leading to inferential deductions.

1.2.2 Premotor cortex: involvement in reasoning based on deductions

In the macaque brain, the premotor cortex (PMC) is a functionally distinct cortical field located between the primary motor area (M1) and the prefrontal areas. It corresponds to the Brodmann area 6, further divided into the ventral and dorsal premotor cortex (PMv and PMd). The premotor cortex is reported to be involved in motor preparation and especially in the synthesis of skilled motor sequences (Wise, 1985). The PMC receives the inputs from the parietal lobes and indirectly from the DLPFC, which is believed to be transmitting them to the primary motor area, M1 (Wise et al., 1992; Fine and Hayden, 2022). Many physiological studies have found that PMC is a heterogeneous frontal area containing distinct sub-regions (Barbas and Pandya, 1989). Previous studies have accounted the role of PMC in set-related activity in motor-preparation and signal the arm movement directions during the reaching tasks (Weinrich and Wise, 1982; Kurata and Wise, 1988; Caminiti et al., 1991). Different sub-areas in PMC partake differential roles in motor control; PMd is more important than PMv in conditional motor behavior and plays a role in preparation for forthcoming movements. In contrast, the PMv is more specialized for a role in the execution of visually guided movements (Kurata and Hoffman, 1994). First accounts of the role of PMd has been limited to the code the movement-related parameters such as the set related activity, the direction and the speed of the movement, action preparation by temporal structure in cortical activity and other aspects of motor preparation, and subsequently the execution (Weinrich and Wise, 1982; Kurata and Wise, 1988; Caminiti et al., 1991; Churchland, 2006).

Another role of PMd widely discussed in the literature is action planning. Action or motor planning refers to the preparation of the behavioral outcome when more than one option or piece of information is presented to the subject, and this information is to be integrated to plan the execution of an action. As an experimental model for action planning, a behavioral paradigm was developed by Hoshi and Tanji, which required the monkeys to learn the cue response relationship in a two cue task (Hoshi and Tanji, 2000). The first cue was the arm to be used and the second cue was the location of the target on the screen. Hence, making a decision required the monkeys to execute a reaching movement by remembering the information about the first cue, which was separated by a delay from the second cue. The authors finally reported different populations of neurons in PMd, encoding both the instructional cues and the integration of the information required to plan and execute the action. In another study, the experimental model of action planning was designed using multidirectional choices, and the correct target was to be chosen as a result of the consequent non-spatial cue (Cisek and Kalaska, 2005). The authors have reported that initially, the PMd neurons represented potential reach directions if one of them was near their preferred location and subsequently represented the direction of the selected reach target. They proposed that multiple reach options are initially specified in the PMd and then gradually eliminated in competition for overt execution, while the response choice was still represented by PMd activity.

In addition to the response and visual target information during an action selection task, abstract rules during a task performance can also be represented by the PMd activity similar to PFC (Wallis and Miller, 2003). On the contrary to the assumption of a top-down flow of information from frontal areas to PMd, this study reports a prolonged and earlier representation of abstract task rules when compared to PFC. However, the information of the individual visual cues was only encoded by the PFC neurons. This opens the possibility of involvement of PMd in higher cognitive functions while representing the abstract variable, such as the task rules in addition to the behavioral response and the action execution.

Further elaborating the role of PMd in a more demanding cognitive process, the recent study by (Mione et al., 2020) has illustrated the manipulation of the PMd neuronal activity during a TI task. The monkeys were trained using a 6-item series and then tested for the transitive problems as the potential targets (target-distractor pair) were presented on two distinct spatial locations on the screen. The neuronal activity was studied during the delay in the preferred spatial position of the neurons. The neuronal activity, in turn, reflected the difficulty in making the decisions as an effect of symbolic distance (SDist)[1], i.e., the correct target was encoded by the neuronal population earlier if the decision was easy (higher SDist). In contrast, high latency of target selection was observed when the test pair was characterized by more difficult decisions (lower SDist). These results emphasize the SDE in the target selection latencies and the percentage of neurons participating in this selection.

[1]From here, while referring the published experimental works, the acronym SDsit refers to the Symbolic Distance Effect, referred elsewhere as SDE.

1.2.3 Acquisition and manipulation of the mental schema during TI

It is evident from the previous sections that the transitive inference task is an experimental paradigm that can be used to study the mental and neuronal correlates of deductive reasoning in many species. The literature aimed at explaining the mechanisms of TI provides an insight into how the mental model is created and manipulated during task performance. A vast literature is available on the involvement of various neural circuits involved in TI (learning and test). However, from a neurophysiological perspective, limited research is conducted to address the role of more than one brain area in this type of task where the decision is guided through a mental model. With this pretext, the next section of this thesis presents a comparison of *"Contribution of the Monkey Prefrontal and Premotor Dorsal Cortex in decision making during a Transitive Inference task",* which is Study 1 in chronological order. This study highlights the different timing of PFC and PMd in the terms of target selection while the monkey engages in decision making during the TI task. The decision making in this task is hypothesized to be driven by the already acquired mental schema. Consequently, after exploring the interplay of these two areas reported to be involved in TI processes in the previous literature, we study the neuronal basis of learning during a TI task in the Prefrontal cortex neuronal activity and how does the PFC activity modulate as the animal traverses from learning to testing. This work is indexed as Study 2, titled *"Neuronal encoding of ranked items in primate prefrontal cortex during different phases of a transitive inference task"*.

Study 1. Different Contribution of the Monkey Prefrontal and Premotor Dorsal Cortex in Decision Making during Transitive Inference Task

Abstract

Several studies have reported similar neural modulations between brain areas of the frontal cortex, such as the dorsolateral prefrontal (DLPFC) and the premotor dorsal (PMd) cortex, in tasks requiring encoding of the abstract rules for selecting the proper action. Here we compared the neuronal modulation of the DLPFC and PMd of monkeys trained to choose the higher rank from a pair of abstract images (target item), selected from an arbitrarily rank-ordered set (A>B>C>D>E>F) in the context of a transitive inference task. Once acquired by trial-and-error, the ordinal relationship between pairs of adjacent images (i.e., A>B; B>C; C>D; D>E; E>F), monkeys were tested in indicating the ordinal relation between items of the list not paired during learning. During these decisions, we observed that the choice accuracy increased and the reaction time decreased as the rank difference between the compared items enhanced. This result is in line with the hypothesis that after learning, the monkeys built an abstract mental representation of the ranked items, where rank comparisons correspond to the items' position comparison on this representation. In both brain areas, we observed higher neuronal activity when the target item appeared in a specific location on the screen with respect to the opposite position and that this difference was particularly enhanced at lower degrees of difficulty. By comparing the time evolution of the activity of the two areas, we observed that the neural encoding of target item spatial position occurred earlier in the DLPFC than in the PMd.

Keywords: transitive inference task, prefrontal cortex, premotor cortex, monkey, decision making

Accepted in Neuroscience, Preprint is available *here*

2.1 Introduction

When reaching a target, visual information about the target properties and location must be transformed into spatially oriented motor acts. Cortical circuits behind these transformations embed neurons that show spatial preference, i.e., higher neuronal activity for a specific target position compared to others (Wise et al., 1992; Caminiti et al., 1998; Ferraina et al., 2001; Lebedev and Wise, 2001). When more potential targets are simultaneously presented, neurons with different spatial preferences compete for signaling the proper target location and reaching direction (Cisek and Kalaska, 2005). An open question is whether and how perceptual or cognitive factors affect this decision-making process and subtending neuronal activity. The manipulation of perceptual variables, such as visual discriminability, demonstrates that the difficulty in encoding the target position was reflected in less sharp spatial preference in different brain areas (Coallier and Kalaska, 2014; Coallier et al., 2015; Chandrasekaran et al., 2017). However, how cognitive variables influence spatial preference-related activity in brain areas involved in visuomotor transformation is still poorly investigated. It has been recently demonstrated that in the dorsal premotor cortex (PMd), a brain area with a key role in visuomotor transformation in primates (Johnson et al., 1996; Boussaoud et al., 1998), neurons express their spatial preference depending on the cognitive difficulty in selecting the target when simultaneously presented with a non-target (Mione et al., 2020). In the quoted work, by using a Transitive Inference (TI) protocol, monkeys were first required to create a mental representation of a rank-ordered set of visual items as A> B> C> D> E > F and then to use this representation to select the higher-ranking item (target item) within all possible pairs by performing a reaching movement. In different trials, the target item was randomly presented on the left or the right side of a computer screen and paired with a non-target-item presented at the opposite spatial position. Within this experimental design, cognitive difficulty was modulated by pairing target and non-target items as a function of their proximity to the item in the mental representation of their ordinal position. The degree of proximity of pairs of items is quantified by their difference in rank and referred to as the symbolic distance (SDist) effect at the behavioral level. Depending on the symbolic distance, target selectivity for item B - for example - was easier when paired with non-target item E (higher distance between items on the mental representation corresponding to SDist = 3) and more difficult when paired with non-target item C (lower distance between items on the mental representation corresponding to SDist = 1). The authors found that this cognitive difficulty affected the neural spatial preference (spatial selectivity) in PMd.

Several neurophysiology studies have revealed comparable neural activation between the PMd and DLPFC while encoding a given task-relevant variable, thus suggesting an overlapping competence of the two brain areas (Cromer et al., 2011; Yamagata et al., 2012; Fine and Hayden, 2022). It is known that the prefrontal cortex can flexibly encode different task-relevant variables (Donahue and Lee, 2015; Fusi et al., 2016; Astrand et al., 2020), including the position of the target in oculomotor delayed visual search and delayed-response tasks (Iba and Sawaguchi, 2002). Here, we first asked if target position

selectivity of the DLPFC emerges during the decision process of a TI task, and then we tested for differences between the DLPFC and PMd.

We observed that the spatial selectivity of both DLPFC and PMd neurons was modulated by cognitive difficulty in target selectivity. Importantly, the comparison between the time evolution of neuronal activity in the two brain areas revealed that the selection of target position occurred with different timings in the DLPFC and PMd. In this work, in line with previous studies (Cromer et al., 2011; Yamagata et al., 2012), we support the idea of a tight interplay between the lateral PFC and PMd in the target position encoding for action execution.

2.2 Materials and Methods

2.2.1 Subjects and Data Acquisition:

Animals: Neuronal activity was recorded from the DLPFC and the PMd of three male rhesus monkeys (Macaca mulatta), weighing 5.50 kg (Monkey 1), 6.50 kg (Monkey 2), and 10.0 kg (Monkey 3) respectively, while performing a TI task. Monkey 1 and Monkey 2 were used to record the data from DLPFC as reported in (Brunamonti et al., 2016); Monkey 1 and a third monkey, Monkey 3 (Mione et al., 2020; Monkey 3 is referred as Monkey 2 in the referred article) were used for the PMd recording.

DLPFC Recording: In Monkey 1 and Monkey 2, the cells in the dorsal area of the prefrontal cortex (DLPFC; Figure S1) were targeted, and the neural activity from these cells was recorded extracellularly using a five-channel multielectrode recording system (Thomas Recording, Germany) acutely and in different sessions. The recording chambers were surgically implanted in the left frontal lobe at stereotaxic coordinates: anterior-32 and lateral-19 in Monkey 1 and anterior-30 and lateral-18 in Monkey 2 along with head restraining devices (Brunamonti et al., 2016). At the end of the neurophysiological experiment, the location of the electrodes was confirmed by visual examination following the surgical opening of dura for the implantation of a chronic array in Monkey 1 (given the following recording from PMd neurons), while in Monkey 2, the electrodes' location was confirmed using a structural MRI scan.

PMd Recording: Neural activity was recorded extracellularly from the left PMd of Monkey 1 and Monkey 3 (Mione et al., 2020; Figure S1) using chronic electrode arrays (96-channels; Blackrock Microsystems, Salt Lake City, Utah).

The surgical procedures in all three monkeys were performed under aseptic techniques while keeping the animal under general anesthesia (1-3% isloflurane-oxygen, to effect).

The monkeys were housed and cared for following the European (Directive 2010/63/EU) and Italian (D.L. 26/2014) laws, regulating the use of nonhuman primates in scientific research. The Italian Ministry of Health approved the research protocol. Housing conditions and experimental procedures were in line with the Weatherall report (use of nonhuman primates in research).

Behavioral data recording and task implementation: The task was controlled using the Cortex Software package (https://nimh.nih.gov/) and administered by presenting the task stimuli on a touchscreen (MicroTouch, sampling rate of 200 Hz) connected to the computer through a serial port to detect the response. An RX6 TDT recording system (Tucker-Davis Technologies, Alachua, FL, USA) was employed during the DLPFC recording sessions, which was synchronized to the behavioral events to detect and record neuronal activity during each trial. During the PMd recording sessions, an RZ2 TDT system (Tucker-Davis Technologies, Alachua, FL, USA) was used, since a higher number of simultaneously recorded channels were dealt with.

2.2.2 Test stimuli and task design

For this study, at the beginning of every session, six stimulus images were randomly selected from a database of 80 abstract black and white images (16^o X 16^o visual angle, bitmaps) and arbitrarily ordered to form a ranked series (Figure 2.1A). To avert the familiarity of the stimulus/rank association, any of the stimuli were not repeated or assigned to the same rank for a significant number of consequent sessions (Brunamonti et al., 2014, 2016; Mione et al., 2020). The monkeys were trained to learn the relationship among all the items of this ranked series.

Each experimental session (for both DLPFC and PMd neural recordings) comprised a learning phase, requiring the monkeys to learn the novel relationship between all the adjacent items (Figure 2.1B: SDist1) in the ranked series, and a test phase in which the monkeys were asked to infer the relationship between novel pairings of nonadjacent items (Figure 2.1B; SDists >1). The learning phase was accomplished by means of two different methods: 1) sequential learning and 2) a chained learning procedure, as reported in our previous works (Brunamonti et al., 2016; Mione et al., 2020). More specifically, in the sequential learning sessions, monkeys were required to progressively learn the reciprocal rank order of pairs of items adjacent in the sequence, while in the chained learning procedure, monkeys were required to link two lists of 3 rank-ordered items previously acquired by sequential learning.

Sequential learning was implemented in two steps: learning phase 1 and learning phase 2. During learning phase 1, the monkeys were presented with the pairs comprising adjacent items sequentially, and they were required to identify the higher ranking item by trial and error in blocks of 15 (Monkey 1: DLPFC recording) or 20 (Monkey 2: DLPFC recording; and Monkey 1 and Monkey 3 PMd recording) trials. Each block was repeated until the monkey achieved a performance of at least 90% (DLPFC recording) or 80% (PMd recording) for the pair. Once the desired performance was reached for every pair in the series, learning phase 2 followed, where the previously experienced pairs were presented in a random order in larger blocks of trials, and a different criterion (> 60% correct trials) was used.

In contrast, during the chained learning procedure, the six-item list was divided into two smaller three-item lists (A>B>C and D>E>F). The rank order of the two three-item lists was learned independently by the sequential learning method in separate blocks until the monkeys achieved a criterion of at least

80% correct trials. The two lists were then linked by learning the association C>D in blocks of 20 trials. The chained learning procedure allowed us to study the manipulation of the ranked order of the series according to the newly acquired information of the linking pair C>D; hence, the rank of the items in the second series was redefined in the unified list, supporting the behavioral strategy of inferential reasoning.

Both learning procedures allowed the monkeys to perform the test phase with a performance significantly above the chance level. We have previously reported that the performance in the test phase after the two different learning methods was comparable (Mione et al., 2020).

For the DLPFC experiment, all the sessions were recorded with Monkey 1 and Monkey 2 using sequential learning only (see Brunamonti et al., 2016 for further details), whereas during the PMd recording, Monkey 1 and Monkey 3 were tested for 7 sessions each using different learning procedures: chained-list learning in 6 (Monkey 1) and 4 (Monkey 3) sessions and sequential learning in 1 (Monkey 1) and 3 (Monkey 3) sessions (see Brunamonti et al., 2016; Mione et al., 2020 for further details).

In the test phase, all the possible pairs of items were presented in a random order (Figure 2.1B; SDist1 – SDist5). Each pair was presented at least 14 or 18 times during the DLPFC and PMd experiments, respectively, with an equal probability of the target item being presented on the left or the right position of the screen.

The time course of each trial was identical for the learning phase and the test phase during all the recording sessions from the DLPFC and PMd (Figure 2.1C). At the beginning of each trial, a red dot (central target) was presented at the center of the screen, and the monkey had to respond within 5 s by pressing a button fixed on the monkey chair (DLPFC sessions) or by touching the red dot on the screen (PMd sessions; as depicted in Figure 1C) until the appearance of a pair of items on the screen. The monkey was required to maintain the touch (or the button pressed) for a random variable Delay period (600-1200 ms) after the Pair Onset until the red spot disappeared from the screen (Go Signal). The Go Signal instructed the monkeys to select (to reach) the higher-ranking item on the screen to obtain the reward.

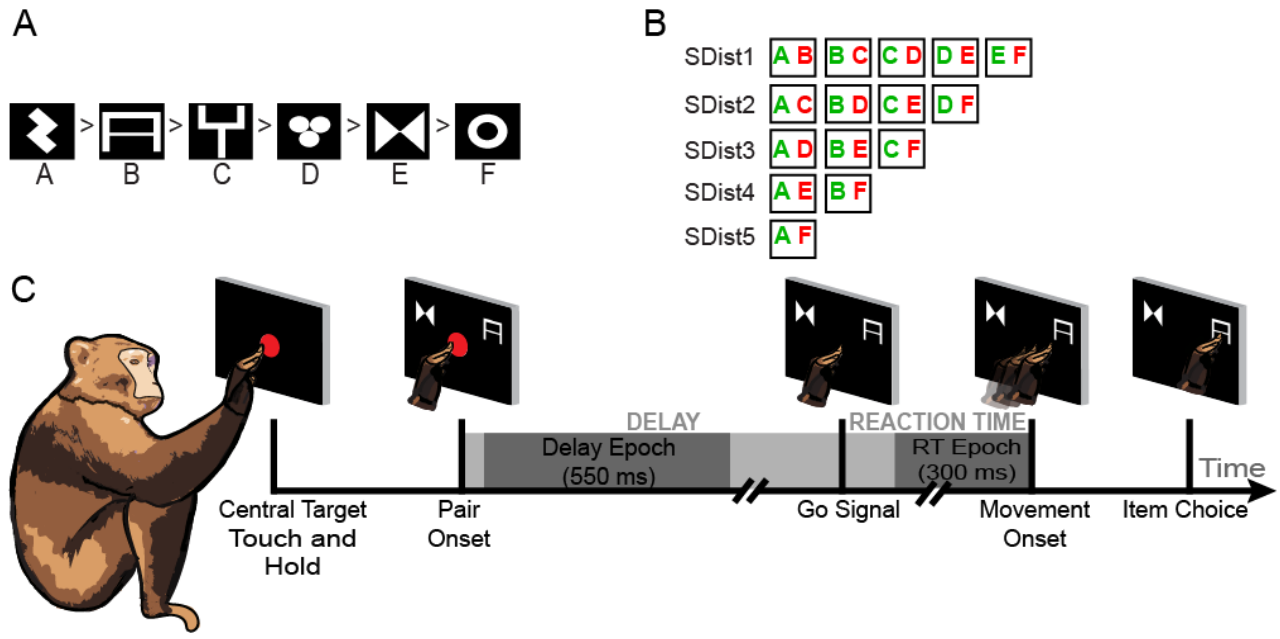

Figure 2.1. Task design and Analysis Epochs: A. An example of a 6-item ranked series chosen at the beginning of the experiment. The letters under each symbol are used here for illustrative purposes only. **B.** All the possible combinations of pairs from the items of the ranked series and their symbolic distances (SDist) associated with each combination; target items represented in green and non-target in red, following the link of each symbol with a letter as in A. **C.** Time course of a single trial during each session. The epochs used for analysis of neuronal activity are highlighted (dark grey).

2.2.3 Data Analysis

Selection of DLPFC and PMd recording sessions:

One of the goals of the present work is to compare the temporal evolution of the neuronal encoding of the target position between the DLPFC and PMd while performing a TI task. Since this comparison was performed by analyzing the neuronal activity recorded in different experimental sessions, we first assessed that differences in the time evolution of the brain activity between the two areas were independent of different levels of accuracy and response time of monkeys in different sessions. To this aim, we evaluated the mean performance and the RTs of the DLPFC and PMd sessions from all three animals and observed that sessions from both experiments were characterized by significantly different RTs (Table 2.1). Additionally, we observed that the RTs of monkey 1 from the DLPFC (296 ms) and the PMd (393 ms) sessions were significantly lower than those of monkey 2 in the DLPFC sessions (386 ms) and monkey 3 in the PMd sessions (437 ms). To account for these differences, in the following analyses, data obtained from Monkey 1 were analyzed independently from those obtained in recording sessions with Monkey 2 and Monkey 3. To compensate for the differences between RTs from DLPFC and PMd sessions in each comparison, we calculated a range of RTs from PMd sessions ($\mu \pm 3\sigma$, where μ is the mean and σ is the standard deviation). As there were only 7 sessions recorded from the PMd of Monkey 1 and Monkey 3, we selected all the sessions recorded from PMd and selected a subsample of

DLPFC sessions (14 sessions from Monkey 1 and 22 sessions from Monkey 2) conforming to the defined range of RTs. As a result of this selection, we obtained comparable RTs between Monkey 1 DLPFC and PMd sessions (all ps>0.05), Monkey 2 DLPFC, and Monkey 3 PMd sessions (all ps> 0.05; see Table 2.1 for details).

	DLPFC	**PMd**	**Two- sample t test**
	All sessions; both animals	**All sessions; both animals**	
Average accuracy (SD)	0.89 (0.07)	0.85 (0.06)	t (105)= 1.89, p=0.06
Average Reaction Time (SD)	346 (91) ms	411 (53) ms	t (105)= -2.06, p=0.01
	Monkey 1 (selected sessions)	**Monkey 1 (all sessions)**	
Average accuracy (SD)	0.90 (0.05)	0.86 (0.08)	t(19) =1.28, p=0.21
Average Reaction Time (SD)	350 (75) ms	386 (32) ms	t(19) = -1.99, p=0.24
	Monkey 2 (selected sessions)	**Monkey 3 (all sessions)**	
Average accuracy (SD)	0.92 (0.10)	0.85 (0.09)	t(1,27) = 1.77, p=0.08
Average Reaction Time (SD)	433 (46) ms	437 (60) ms	t(27) = -0.19, p=0.85

Table 2.1: Comparative analysis of average behavior average behavior across PFC and PMd sessions, before and after selection of sessions; SD-Standard Deviation

Behavioral correlates of TI at test: We first investigated whether the behavior during the selected sessions from DLPFC (Monkey 1: 14; Monkey 2: 22) and PMd (Monkey 1: 7; Monkey 2: 7) recordings was modulated by the SDist. This analysis was performed to assess whether the monkeys' ability to select the target item over the simultaneously presented nontarget item depends upon the distance of the two items in their mental representation. To this aim, we tested whether the probability of selecting the correct item significantly increased and the corresponding RT significantly decreased with increasing symbolic distance. To further investigate if the monkeys employed the mental models to solve the task during the selected sessions, we calculated the performance and the normalized reaction time for the selected DLPFC (Monkey 1: 14 and Monkey 2: 22) and all the PMd (Monkey 1: 7 and Monkey 3: 7) sessions for each pair comparison. Using a linear regression, we analyzed if the performance and the RTs for individual item comparisons correlated with the SDist (Figure S2).

Neuronal correlates of TI in the test: We studied 141 neurons from the DLPFC (Monkey 1: 56, Monkey 2: 85) and 186 neurons (Monkey 1: 59, Monkey 3: 127) from the PMd obtained during the test phase of the TI task of the selected recording sessions. The data analysis was performed on trials in which the

monkey correctly selected the position of the target item. Error trials in which the monkey selected the non-target items were not considered in the following analyses. To address whether the activity of DLPFC neurons correlated with the difficulty in selecting the position of the target item, we first studied spatial preference for the target that emerged in the neuronal activity of DLPFC, and then we tested whether this preference was modulated by the SDist. As a further step of the analysis, we compared the pattern of neuronal activity in the DLPFC and PMd to evaluate how it differed between the two brain areas during different epochs of the task. In doing so, we studied the neuronal activity from each neuron during two task epochs, 1) the Delay epoch, lasting from 50 ms to 600 ms after the Pair Onset; 2) the Reaction Time epoch, lasting for 300 ms before the Movement Onset (Figure 2.1C). For each neuron, we calculated the mean spike rate from the correct trials corresponding to each of the two target positions (left and right) at every SDist (SDist1-SDist5). Furthermore, we normalized the mean spike rate across different task conditions by applying a z score transformation.

To quantify the degree of preference of each neuron for the left or right target position, we first represented the neuronal activity as a point in a 2-dimensional space having the neuronal activity for the right and left positions of the target as x and y coordinates, respectively (Figure 2.3, 2.4). Then, we computed the shortest distance (D_n) of each point from the equality line (representing a preference or a lack of preference for any of the two target positions) as follows:

$$Dn=\frac{Right_n - Left_n}{\sqrt{2}}$$

where $Left_n$ and $Right_n$ are the coordinates of the n^{th} neuron in the defined space, representing the normalized mean neuronal activity during the trials with the target located in the left and right positions, respectively. D_n represents the difference between the neuronal activity between these two target positions in this graphical context (Figure 3B), where the negative values represent the neuronal preference for the left target position and positive values for the right target position. A high magnitude of D_n (positive or negative) indicates a greater degree of preference for one of the two positions of the target, which we further utilized to identify the neurons showing a significant target position preference. Across the population of neurons from each area, we calculated the maximum range of variation during the two analysis epochs: $D_{population} = (D_{n\_max} - D_{n\_min})$. Then, we defined a neuron to be selective for the left or the right target position if the corresponding positive or negative value D_n was lower ($D_n < 0$) or higher ($D_n > 0$) than 10% of the total range of excursion ($D_{population}$). To study how the preference for the target position was modulated by the task difficulty, we first identified the DLPFC and PMd neurons displaying a target position selectivity at SDist5 (the easier condition of the task), and then we observed how this selectivity changed across other SDists. We used a linear model fit to test whether the target position selectivity was significantly modulated by the rising SDist for each target position (left and right).

We applied a Receiver Operating Characteristic (ROC) analysis on neuronal activity recorded during the selected sessions to study the time course of target position selectivity in DLPFC and PMd

((Thompson et al., 1996; Mione et al., 2020)). Once the preferred target position of each neuron at SDist5 was identified, we computed the area under the ROC curve (auROC) in consecutive time bins in a time epoch starting 500 ms before to 1300 ms after the pair onset using a moving time window of 200 ms with a 20 ms step. Thus, for each time window of every neuron, we obtained a probabilistic measure of encoding the target when it was presented in the preferred position compared to the opposite position. We estimated the latency of target position discrimination by calculating the time when the auROC value crossed the threshold of 0.6 for 60 ms (3 consecutive time bins) in the trial time ranging from 80 ms to 1300 ms after the Pair Onset. We repeated this estimate for the comparisons at SDist lower than 5 to test if the latency of spatial discrimination changed in pairs comparisons of increasing degrees of difficulty in both, DLPFC and PMd. The auROC values were calculated for a balanced number of trials for all the task conditions, corresponding to the minimum number of correct trials across all the task conditions. On average, the number of trials for each position of the target was 17 (SD=5) for DLPFC sessions and 31 (SD=16) for PMd sessions.

To account for the differences in RT detected in Monkey 1 and the other two monkeys (see previous section), we performed latency estimates of target position selectivity in different groups of neurons: 1) neurons obtained by Monkey 1 in which the RT in DLPFC (47 neurons) and PMd (55 neurons) recording sessions was not significantly different; 2) neurons obtained by Monkey 2 in DLPFC (79 neurons) sessions and neurons recorded in Monkey 3 PMd (119 neurons) sessions with RT were not significantly different.

The latency of target position discrimination in neurons measured in Monkey 1 and those measured in Monkey 2 and Monkey 3 were analyzed separately. To test for the differences between latencies across different task conditions and different areas, we calculated the probability of observing latencies in the initial 75% of the distributions (< 900 ms). Consequently, we applied a Kolmogorov Smirnoff test to identify the interarea differences between these probabilities if any. At test was used to compare the interarea differences between the average latencies across the different SDists. To explore further how the neuronal populations of two areas encode target positions with varying difficulties, we computed the fraction of cells showing sustained coding for the target position (auROC>0.6 for more than 70% of the total time) as a function of SDist. The differences in the measures between the two areas were tested using a Kolmogorov Smirnoff test. All data analyses were performed using custom-made functions developed in MATLAB (The MathWorks) and Wolfram Mathematica.

2.3 Results

2.3.1 Choice difficulty modulates the ability to select the target position during the TI task

The accuracy and RT for target position selection exhibited a significant SDist effect during the pair comparisons of the test phase in both the DLPFC and PMd recording sessions (Figure 2.2, Figure S2). A linear regression analysis revealed a significant increase in the proportion of correct to incorrect

choices and a decrease in the RT with the rising SDist (see table 2.2 for details on the regression analysis) for each monkey. These results are in line with the hypothesis that, at the end of the learning phase, ranked items are arranged on a mental line, and the difficulty in pair comparisons at test depends on the relative proximity of the items' representation on this line (Brunamonti et al., 2011, 2016; Mione et al., 2020).

DLPFC Sessions	**Monkey 1**	**Monkey 2**
Accuracy (left target)	P_{left}=-0.51(SDist)+0.76, p<0.05	P_{left}=-0.037(SDist)+0.80, p<0.05
Accuracy (right target)	P_{right}= 0.50(SDist)+0.78, p<0.05	P_{right}=0.022(SDist)+0.89, p<0.05
RT (left target)	RT_{left}= 0.10(SDist)+0.32, p<0.05	RT_{left}= 0.22(SDist)+0.67, p<0.01
RT (right target)	RT_{right}= -0.15(SDist)+0.42, p<0.05	RT_{right}=-0.20(SDist)+0.60, p<0.01
PMd Sessions	**Monkey 1**	**Monkey 3**
Accuracy (left target)	P_{left}=-0.056 (SDist)+0.74, p<0.01	P_{left}=-0.075 (SDist)+0.66, p<0.01
Accuracy (right target)	P_{right}=0.058 (SDist)+0.71, p<0.01	P_{right}=0.067 (SDist)+0.69, p<0.01
RT (left target)	RT_{left}= 0.46 (SDist)+1.37, p<0.01	RT_{left}= 0.46(SDist)+1.38, p<0.01
RT (right target)	RT_{right}= -0.49(SDist)+1.48, p<0.01	RT_{right}= -0.42(SDist)+1.25, p<0.01

Table 2.2. Linear Correlation Coefficients of SDist with behavior of each monkey during DLPFC and PMd recording sessions

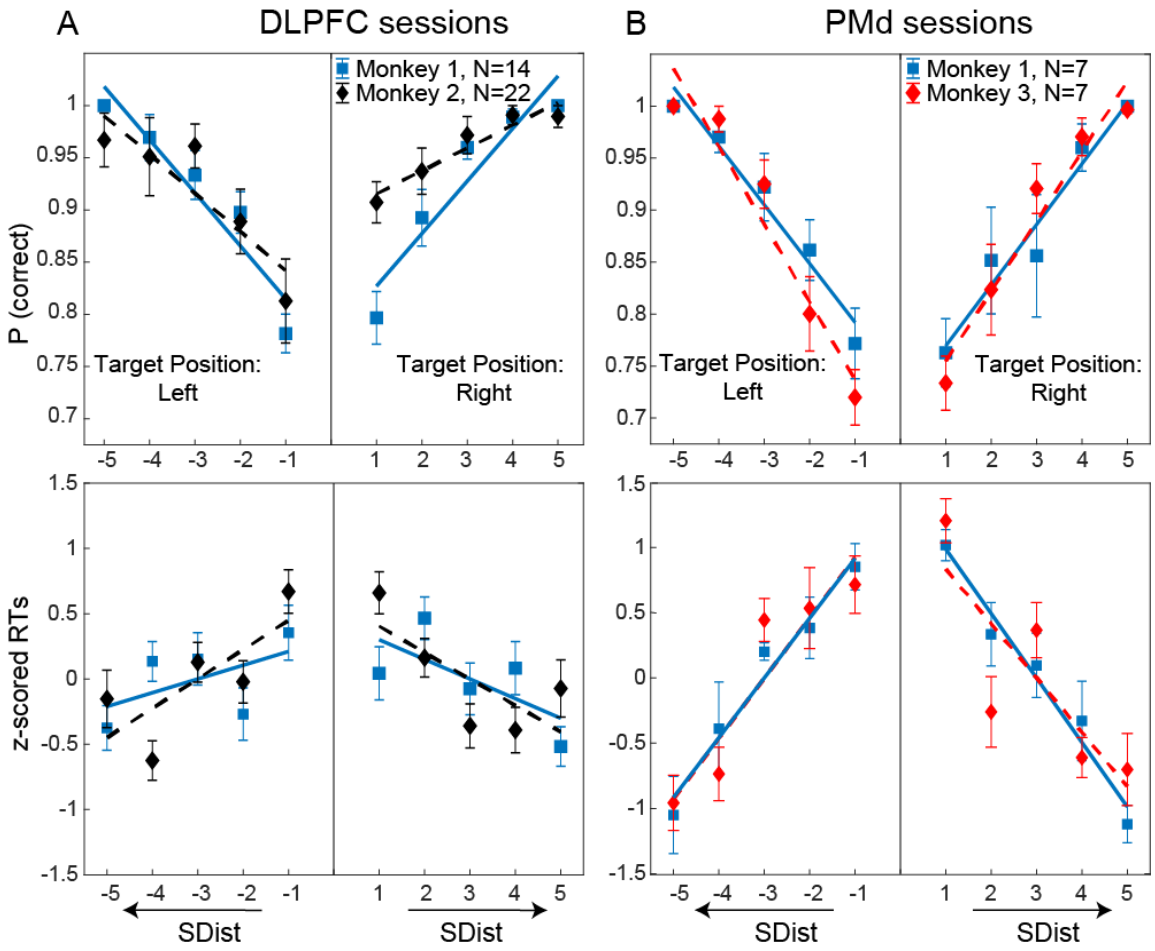

Figure 2.2. Influence of SDist on behavioral performance: Proportion of correct choices (top plots) and corresponding z scored RT (bottom plots) for target selection at every SDist when the target was presented on the left and the right position of the screen during 'N' recording sessions from DLPFC (A: Monkey 1 and Monkey 2) and PMd (B: Monkey 1 and Monkey 3). Squares and diamonds correspond to the average performance and z scored RT, respectively; across the sessions, vertical bars represent the S.E.M. Linear regression fit across sessions is reported in Table 2.

2.3.2 Populations of DLPFC and PMd neurons encode the task difficulty while differentiating between the target positions

Here, we investigated whether the neuronal correlates of target position selectivity in the population of DLPFC (n=141) and PMd (n=186) neurons were modulated by the difficulty of the task.

Figures 2.3 and 2.4 display the scatterplots of the normalized neuronal activity in response to the presentation of the target on the left (y-axis) or right (x-axis) position on the display for each SDist during the Delay (Figures 2.3A and 2.4A) and Reaction Time (Figures 2.3B and 2.4B) analysis epochs. By representing the activity of each neuron as a point in such 2-dimensional space, we quantified the degree of preference of the target position as the distance from the equality line. According to this criterion, a neuron was classified as spatially selective if its distance from the equality line exceeded 10% of the total range of excursion of the distances calculated across all the neurons and SDists. DLPFC

neurons were considered target selective for the left or right position of the target during the Delay epoch, if their distance from the equality line was lower than -0.49 or higher than 0.49, respectively. The same criterion in the RT epoch identified -0.51 and 0.51 as the threshold for left and right target selectivity. Similarly, a PMd neuron was distinguished to be spatially selective if the magnitude of the distance from the diagonal exceeded ±0.54 and ±0.46 during the Delay and RT epochs, respectively. For each neuron, we first identified the left (blue dots) or right (red dots) preference for the target position, and then we tested whether the encoding of the target location changed as the difficulty in pair comparisons gradually increased, i.e., during the pairs comparisons from SDist5 to SDist1.

We quantified the proportion of neurons exhibiting target position selectivity at each SDist. The colored density distributions on the top of diagonals in both Figures 3 and 4 show that the proportion of target position-selective neurons identified in the DLPFC and PMd during the Delay epoch gradually decreased as the difficulty in pair comparisons increased (see Figure 2.3D and 2.4D for details). At the same time, the proportion of neurons not showing a significant target position selectivity gradually increased from SDist5 to SDist1 (gray density distributions). This effect was not observed during the RT epoch in either area.

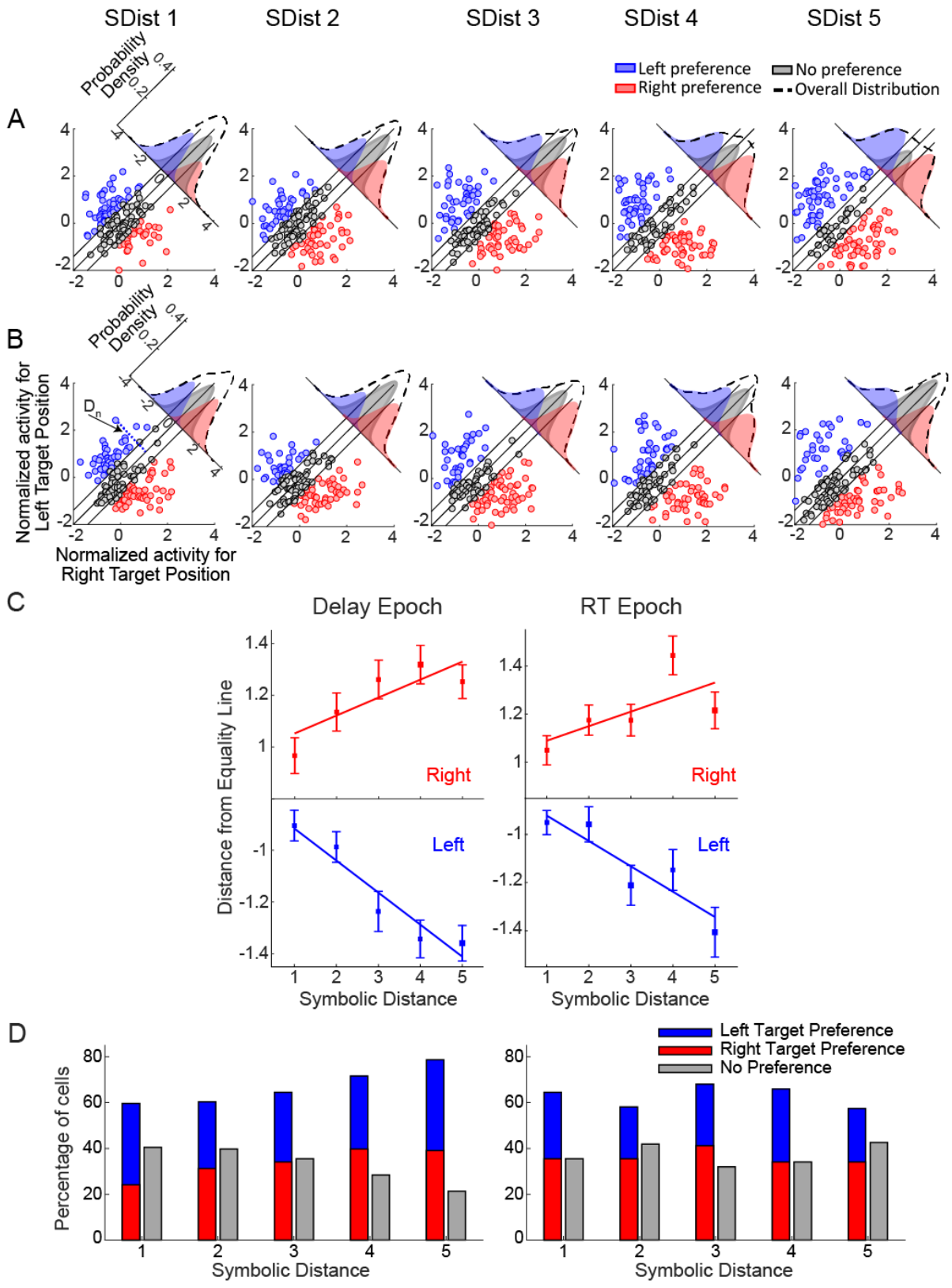

1.

Figure 2.3. Encoding of target position in the population of DLPFC neurons

A-B, Scatter plots comparing the normalized mean neuronal activity from 141 DLPFC neurons during the delay (A) and RT epochs (B), calculated across all the SDists when the target was presented in the left (y-axis) and right (x-axis) positions on the screen. Each dot in the plots represents a single neuron. The preference for the left (blue

dots) or right (red dots) target position of each neuron was detected as its distance (D_n) from the equality line (diagonal in each plot). Neurons with a distance lower than 10% of the total range from the equality line were labeled nonselective for the target position (gray dots). The density plots (dotted line) on the top of each diagonal show the distribution of the spatial selectivity of neurons at each SDist, while the colored density plots represent the corresponding subdistributions for the neurons showing selectivity for left, right, or no target preference. **C.** Mean distances of all the target position selective DLPFC neurons from the diagonal at each SDist for their preferred target positions (left or right), and their linear correlation with the SDist during the delay and RT epochs. They represent the strength of selectivity for left and right target positions exhibited collectively by the neurons, and the regression lines indicate a modulation of target position selectivity during delay (left: $p<0.01$ and right: $p<0.01$) and the RT epochs (left: $p<0.01$ and right: $p<0.01$). Vertical bars indicate the Standard Error of Mean. **D.** Percentage of neurons showing directional target preferences at varying choice difficulties.

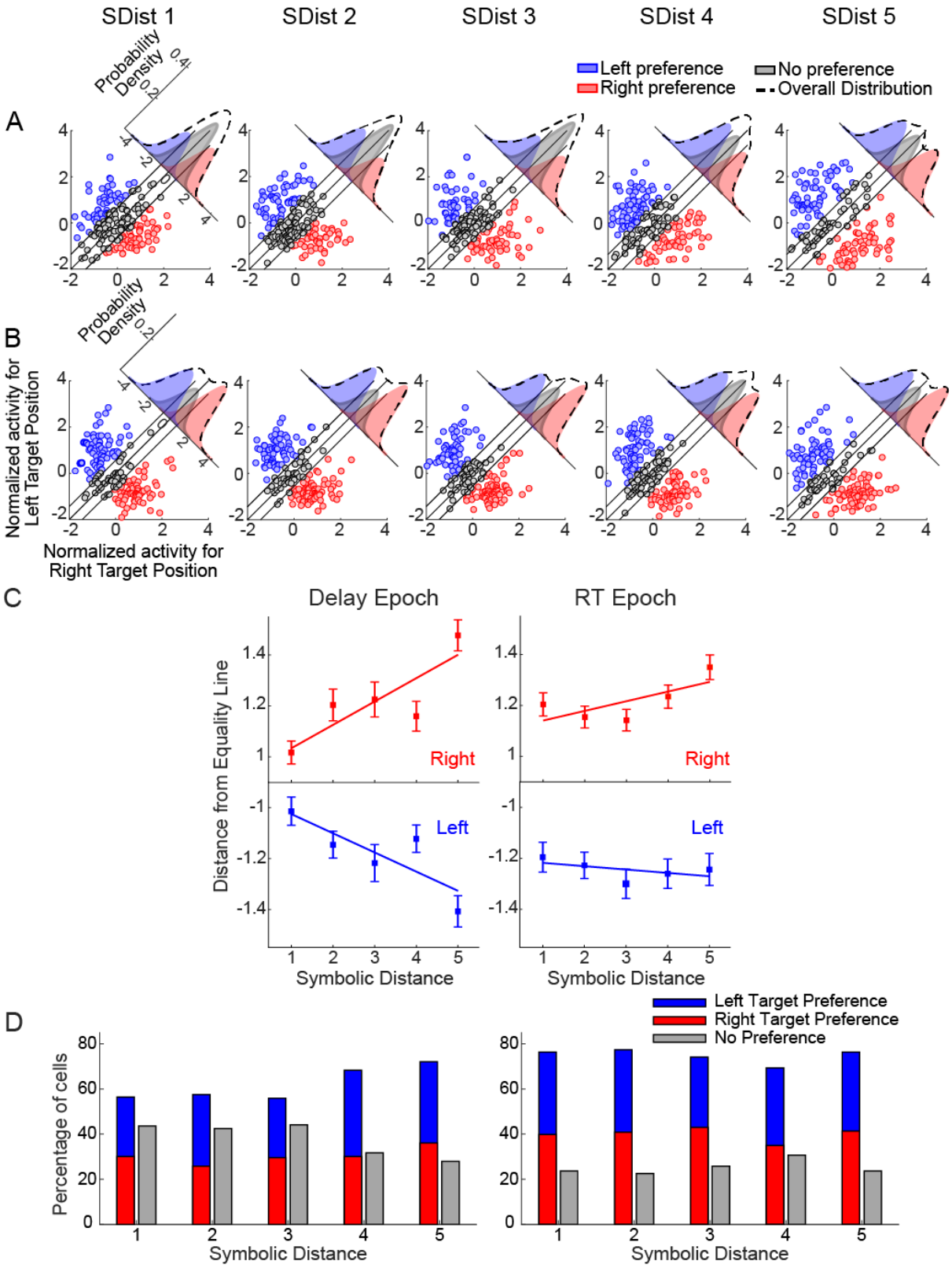

Figure 2.4: Encoding of target position in the population of PMd neurons

A-B, Scatter plots comparing the normalized mean neuronal activity for two target positions in 186 PMd neurons at each SDist during the Delay(A) and RT(B) epochs. The modulation of the neuronal activity is represented with the same codes as in Figure 3. **C.** The plots show the average strength of target position selectivity by overall

target position selective PMd neurons at each SDist during the Delay and RT epochs for left and right target positions. It indicates a linear correlation between the strength of selectivity with the SDist during the Delay (left: $p<0.01$ and right: $p<0.01$), and a weaker modulation for the right target position and no modulation ($p>0.05$) for the left target position during RT by the SDist. **D.** Percentage of the PMd population showing target preferences at different SDists.

We further investigated the strength of target position selectivity as a function of the degree of difficulty in comparing the pairs of items by quantifying the average distance from the equality line for each SDist (leftward and rightward shifting of the blue and red subdistributions in Figure 2.3 A-B and Figure 2.4 A-B). By means of regression analysis, we detected that for both left and right target position selective neurons, the distance from the equality line significantly increased with the increasing SDist in DLPFC neurons during the delay and RT epochs for each of the target positions (left and right: $p<0.$ 01; Figure 2.3C). However, in the PMd neurons (Figure 4C), this effect was mainly detected only in the delay epoch (left and right: $p<0.$ 01) but not in the RT epoch ($p>0.05$). We tested the robustness of these results by detecting that a comparable effect was still present in subpopulations of neurons selected using different criteria (Dn > 5% and Dn > 20%; supplementary Table S1 and corresponding description).

Figure 2.5 (A and B) displays the pattern of activity from four representative neurons from DLPFC and PMd. Figure 2.5A shows the temporal evolution of the activity of two different DLPFC neurons during the time around the Pair Onset (upper panels) and the time around the Movement Onset respectively (lower panels). In these neurons, the average neuronal activity during the corresponding epochs was higher for the right position of the target and increased with increasing SDist. Figure 2.5B displays a similar plot for two PMd neurons. The first of the PMd neurons (upper panels) displays a preference for the left position of the target during the Delay epoch that increased with the growth of SDist, while the second neuron (lower panels) displays a preference for the right position of the target during the time around the movement onset, but this preference was not modulated by the SDist.

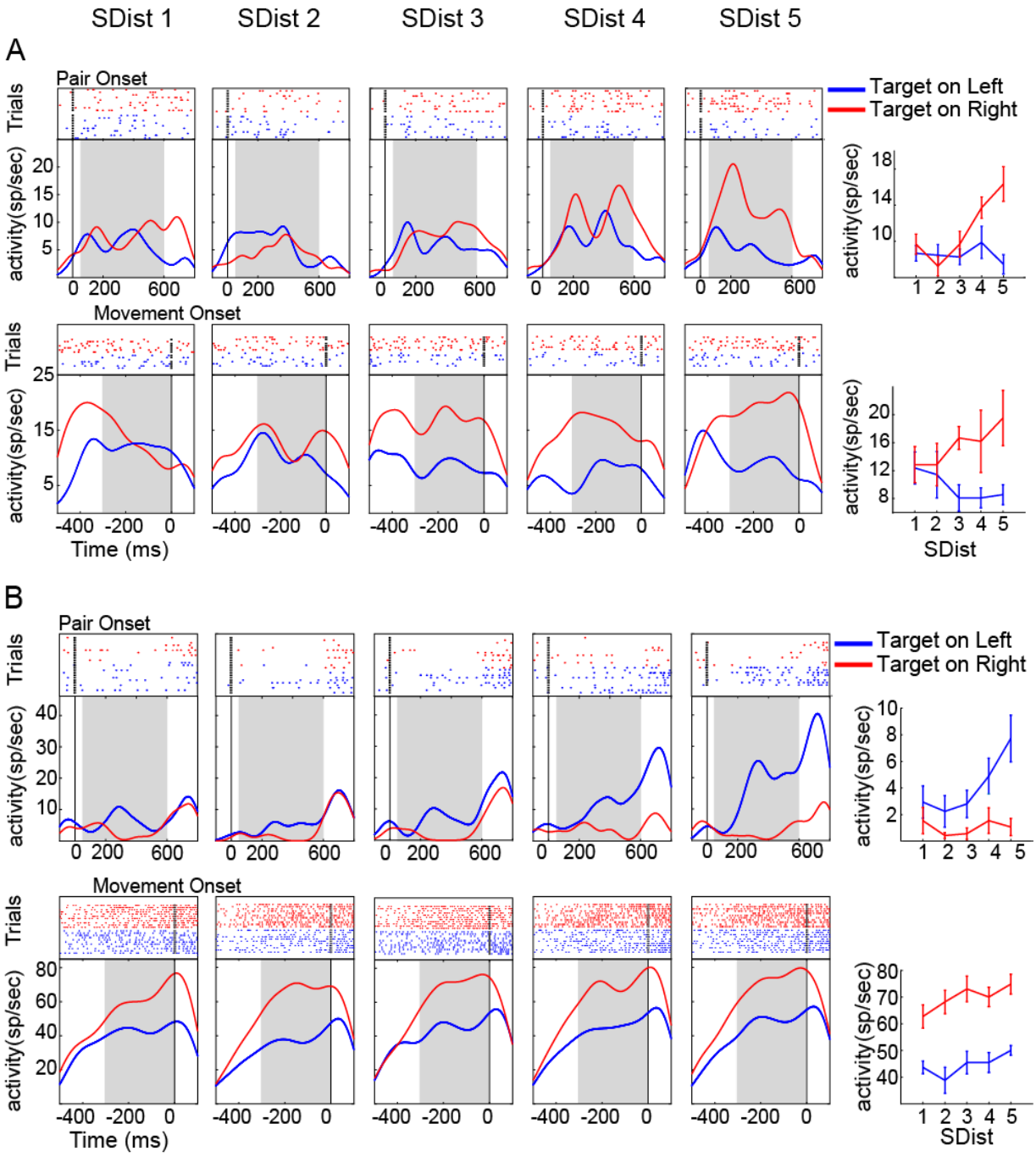

Figure 2.5: Modulation of activity in DLPFC and PMd neurons during pairs comparisons: Time evolution of the neuronal activity of four different neurons recorded from DLPFC (Panel A) and PMd (Panel B), exhibiting a target position selectivity during the Delay epoch (from 100 ms before to 800 ms after the pair onset; first row) and Reaction Time epochs (from 600 ms before to 200 ms after the movement onset; bottom row), respectively. For comparisons at each SDist, the raster plots (upper part) and the corresponding spike density functions (lower part) are plotted for correct trials grouped according to left (blue) and right (red) target positions. The rightmost panels show the mean spike rate as a function of SDist, calculated during the Delay and RT analysis epochs (shaded area). Both the DLPFC example neurons exhibit a preference for the right target position (red) and an increasing difference in neuronal activity for the left and right target positions with increasing SDist. In contrast, only one of the PMd example neurons (top one) modulated its preference for the left position with the rising SDist.

We also observed that the DLPFC example neuron exhibiting a target position selectivity during the RT epoch (Figure 2.5A, bottom panel) displays a decreasing spike rate for the left target position at higher SDist (easier target discrimination). We further evaluated whether this effect was shown by more neurons in the DLPFC population using a linear regression analysis, and we observed that 21/141 (14.8%) neurons studied by us in this area exhibited a negative correlation of neuronal activity with the SDist during at least one of the epochs.

We further asked how many neurons contributed to the encoding of the same target position at each level of difficulty and whether the contribution of a single neuron emerged only for specific levels of difficulty. We observed that a small proportion of DLPFC neurons (8% of all the target position selective neurons) exhibited a preference for the same target position at every difficulty level of the task, while in the PMd, we quantified that 41% of all the target-selective neurons maintained the same directional preferences at every SDist.

To summarize, easier pair comparisons in the TI task are related to the recruitment of a higher percentage of target position selective neurons than for more difficult comparisons, both in the DLPFC and PMd. In addition, the spatial selectivity was found to be stronger for easier pair comparisons. However, in PMd neurons, this trend occurred only during the Delay epoch; in the RT epoch, this selectivity was encoded with comparable strength at each level of difficulty.

2.3.3 The selectivity of the target position occurs earlier in the DLPFC than in the PMd

The previous results indicate that the target position selectivity in both the DLPFC and PMd was influenced by the task difficulty during different epochs of the task. Here, by using an ROC analysis, we explored the time evolution of spatial selectivity of the target position to determine the time at which it occurred in the selected DLPFC and PMd neurons. Figures 2.6A and B show the temporal evolution of the ROC in the time around the pair onset in 47 neurons recorded from the DLPFC and 55 neurons from the PMd of Monkey 1 obtained from the recording sessions with comparable RTs (see methods). Neurons in each plot were sorted according to the time of target position selectivity (see methods for more details). The top histograms on each plot illustrate the distribution of the neuronal estimation of target position selection latencies for each SDist and the corresponding average values. We tested whether the latency in the emergence of the spatial selectivity differed between the two brain areas and whether it depended on the task difficulty by quantifying the probabilities of observing these latencies during the initial 75% (<900 ms) of the distributions at each SDist. We observed a significantly higher probability of finding shorter spatial target selection latencies in the DLPFC than in the PMd (Figure 2.6C - Kolmogorov Smirnoff test; $p<0.05$).

Furthermore, we found that the average target position selectivity latency across all conditions was significantly longer in the PMd than in the DLPFC (DLPFC: 329.2 ms; PMd 403.5 ms; t test: $t(398) = 2.4079$; $p<0.05$). The probability of observing shorter latencies was also found to be higher with the increase in SDist in both areas. We fitted these trends with a linear model and observed a goodness of

fit of 0.78 in DLPC and 0.91 in PMd. Additionally, we detected that the proportion of cells showing sustained encoding for the target position (Figure 2.6D) was greater in the PMd than in the DLPFC (Kolmogorov Smirnoff test; $p<0.01$). This effect did not depend on SDist (goodness of fit: DLPFC $R^2 = 0.08$; PMd $R^2 = 0.53$).

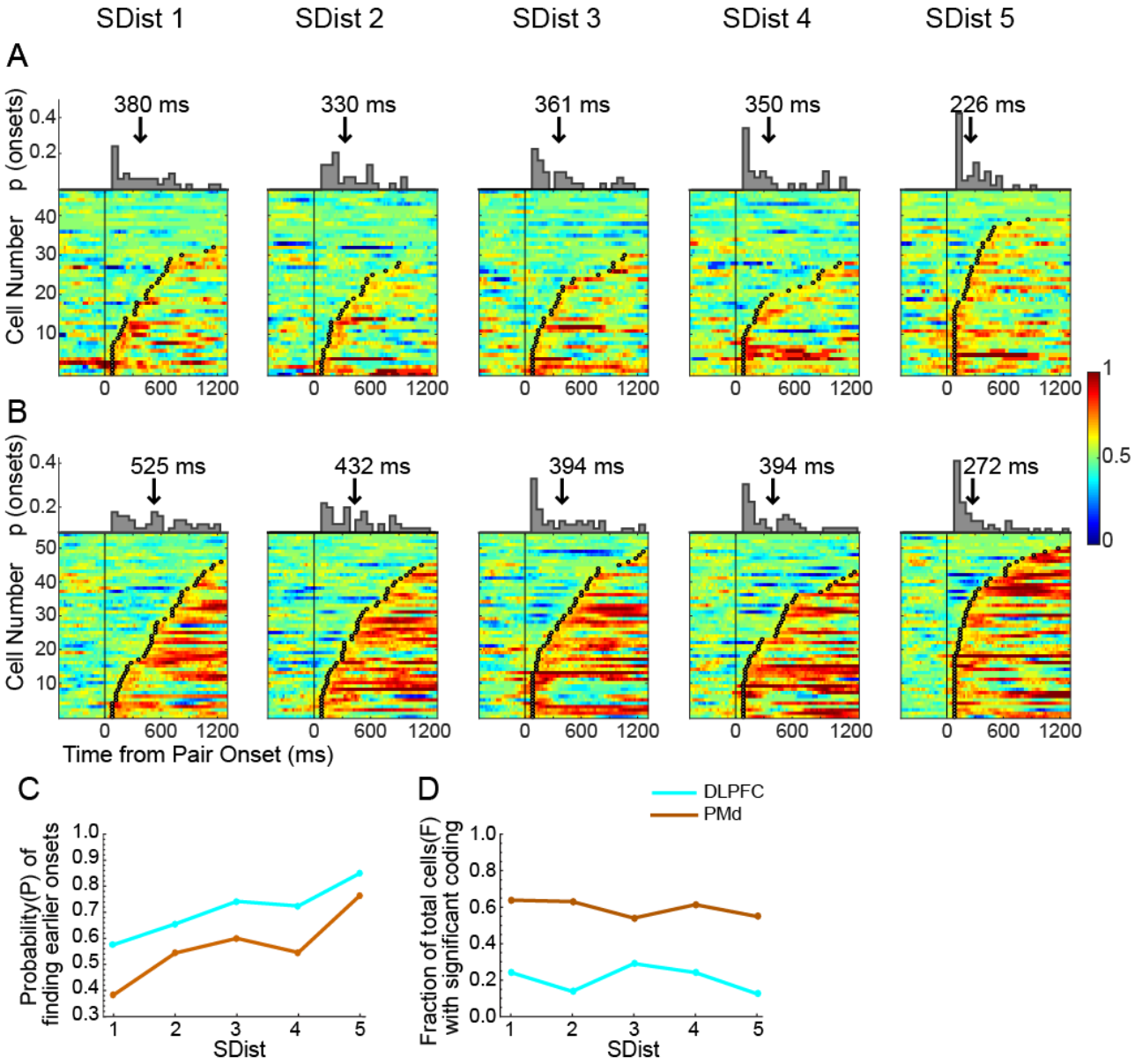

Figure 2.6. Estimate of the time of target position selectivity in the DLPFC and PMd neuronal population from Monkey 1: A-B. Time course of target position selectivity, measured as auROC values between the two target positions, in the time from 500 ms before the pair onset to 1300 ms after it, at each SDist from Population of DLPFC neurons(A) and PMd neurons(B). In each plot, the neurons are aligned sorted to the achievement of the set criterion (crossing the threshold value of 0.6 for 60 consecutive ms), highlighted by the black circles in each row. The histograms on the top show the distribution of these onsets of discrimination between target positions over trial time, and their mean is represented by a vertical arrow for each SDist. **C.** The probability of observing the target selection onsets in the plots (A and B) before 900 ms after the pair onset (75% of the

distribution) as a function of SDist in DLPFC and PMd neurons. **D.** Proportion of total DLPFC and PMd cells in Monkey 1 significantly coding the target position for more than 70% of the total time.

These results were confirmed by comparing the evolution of target position selectivity in the neurons recorded from the DLPFC of Monkey 2 (79 neurons) and PMd of Monkey 3 (119 neurons) during the recording sessions with comparable RT (Figure 2.7A and 7B) across the same trial epoch. We detected a higher probability of finding lower values of target position selection latencies for the DLPFC than for the PMd (figure 2.7C; Kolmogorov Smirnoff test, $p<0.01$), with a significant modulation by the SDist in both brain areas (goodness of fit: DLPFC $R^2 = 0.76$; PMd $R^2 =0.82$). Correspondingly, the mean latencies revealed a significantly earlier target position selectivity in the DLPFC than in the PMd (DLPFC: 338.0 ms; PMd 552.8 ms; t test: $t (741) = 9.2980$; $p<0.05$). The fraction of cells encoding the target position was significantly higher in PMd (figures 2.7D and 2.7E; Kolmogorov Smirnoff test, $p<0.05$) than in DLPFC in the current comparison, with no significant modulation by the SDist (goodness of fit: DLPFC $R^2 = 0.02$; PMd$R^2 =0.49$).

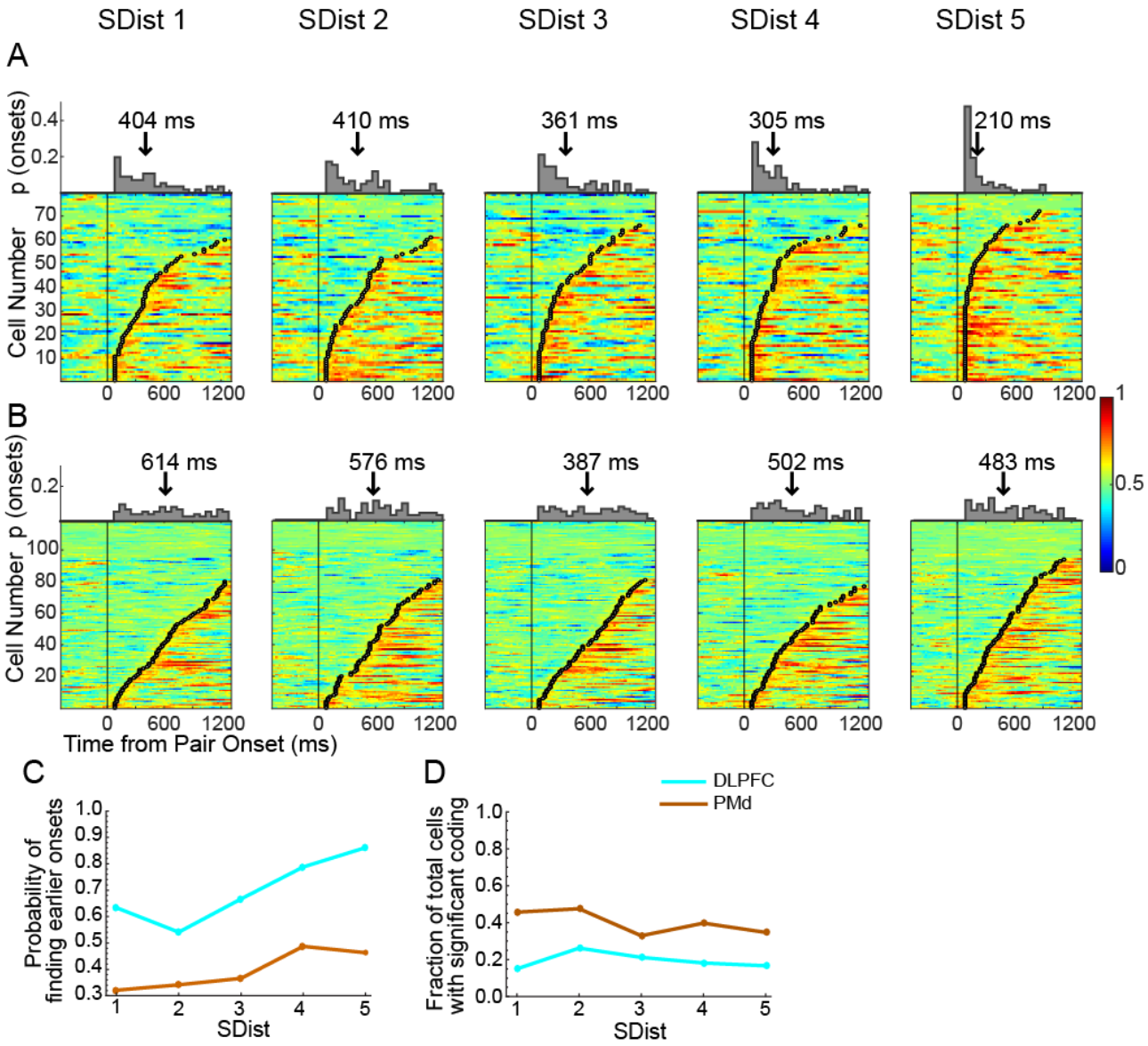

Figure 2.7. Estimate of the time of target position selectivity in neuronal populations from DLPFC of Monkey2 and PMd of Monkey3: Time course of target position selectivity, measured as auROC values between the two target positions, from the duration of 500ms before the pair onset to 1300 ms after it for each SDist for DLPFC neurons of Monkey2 (A) and PMd neurons of Monkey3 (B). C and D: Comparison of the probabilities of finding shorter target selection onsets and the fraction of cells exhibiting significant coding, respectively.

Collectively, these results indicate that both the DLPFC and PMd contribute to target position discriminability decisions in inferential tasks. In both areas, the latencies and the durations of neuron involvement in spatial selectivity depended upon the degree of task difficulty in detecting the target. More importantly, the two areas partake their role in decision making with earlier involvement in target position coding of DLPFC neurons over PMd neurons. PMd neurons maintained the target position encoding for a longer time, with a higher fraction of cells exhibiting sustained coding.

2.4 Discussion

Building mental models by linking isolated events or situations allows appropriate decision making or conceptualizing new knowledge by relying on linked information (Acuna et al., 2002b; Treichler et al., 2003; Jensen, 2017). The spatial structures of these models have been studied in humans and animals (Constantinescu et al., 2016; Jensen et al., 2019; Sheahan et al., 2021) to assess how linked information could be mapped. Recently, it has also been demonstrated how spatially organized models allow the generalization of knowledge across contests (Sheahan et al., 2021) and which computational mechanisms subtend these functions (Brunamonti et al., 2016; Mione et al., 2020). The transitive inference task is one of the experimental approaches used to investigate behavioral and neuronal modulations during this form of decision-making in many brain areas, including frontoparietal and hippocampal regions (Acuna et al., 2002a; Zeithamova et al., 2012; Basile et al., 2020). The recent developments of TI tasks in monkey neurophysiological studies have allowed us to investigate the neuronal correlates of this function with improved spatial and temporal resolution (Brunamonti et al., 2016; Mione et al., 2020; Munoz et al., 2020). A view on cortical neuronal processing subtending the manipulation of spatial models of linked information will provide data to validate or refine the biological reliability of the computations modeled by artificial neural networks (Sheahan et al., 2021). By relying on this approach, we addressed the question of how the difficulty in comparing pairs of items of a learned ranked list modulates the activity of single neurons of both the DLPFC and PMd, two brain areas of the circuit involved in transforming abstract goals in spatially oriented actions (Pezzulo and Cisek, 2016; Grafton and Volz, 2019). The occurrence of the symbolic distance effect in the test session supports our working hypothesis that the symbolic distance effect is consequent to the difficulty arising while making a decision between the rank of two items closely located on the mental representation (Brunamonti et al., 2016; Mione et al., 2020). The analysis of the neuronal data revealed that the degree of difficulty in pair comparisons influenced the spatial selectivity of both DLPFC and PMd neurons. These results confirm our previous observation that the symbolic distance effect modulates the spatial selectivity of PMd neurons (Mione et al., 2020) and document comparable effects in DLPFC neurons.

More specifically, 89% of the DLPFC neurons showed a target position preference, responding with higher levels of activity when the target item was specifically presented at one side of the screen, at least in one of the epochs of the analysis. The proportion of DLPFC neurons preferring the left (45%) and right (54%) directions was comparable and in line with previous studies showing comparable proportions of DLPFC neurons recorded in monkeys performing a motion detection task, while the symbolic distance effect modulated the task difficulty (Lennert and Martinez-Trujillo, 2013). Similar proportions of neurons were observed in PMd (92% neurons selective for the target location; 48% left preference; 52% right preference).

Within this population of target position-selective neurons, we observed an increasing number of neurons exhibiting a preference for the target position in both areas, as the degree of difficulty in

distinguishing between the target and the non-target decreased (Figure 2.3-2.4). However, the distribution of the target position-selective neurons in the two epochs of analysis, as well as their corresponding level of activation, was modulated differently in the two brain areas. More specifically, in the DLPFC, task difficulty modulated the magnitude of neuronal activity both at the time of target presentation and during the time preceding the onset of movement (Figure 2.3C), while in the PMd, task difficulty modulated the magnitude of neuronal activity only at the time immediately following pair presentation. For instance, although PMd neurons encoded the target position in the time preceding the movement onset, the magnitude of the encoding was not modulated by the task difficulty. These results reveal that the activity of PMd is more sensitive to the degree of difficulty of the task soon after the pair presentation but not in the later part of the trial and suggest that the neuronal activity of this area was modulated by the uncertainty in target selection only during the earlier part of the trial. In the time immediately preceding movement onset, the neuronal activity of PMd at lower symbolic distances was comparable to that observed at higher symbolic distances, indicating that the target was already selected at this time.

We also observed differences in the DLPFC and PMd neuronal populations in the way they encoded the effect of task difficulty. In both brain areas, we observed an increasing proportion of neurons recruited for easier pair comparisons; however, while in PMd, approximately 40% of neurons were engaged in encoding the target position at different SDists, only 8% of DLPFC neurons kept encoding the same target position at each SDist. These results reveal that the neuronal population encoding the task difficulty was more heterogeneous in the DLPFC than in the PMd, suggesting a higher level of mixed selectivity properties of this area. Additionally, temporal analysis of target position encoding revealed earlier involvement of DLPFC neurons than PMd neurons. Furthermore, PMd cells, after an initial encoding for the target position that depended on task difficulty, kept encoding the target position with higher sustained activity than DLPFC. However, the fraction of cells exhibiting sustained activity was not modulated by task difficulty in either brain area (Figure 2.6D-2.7D).

All these results are in line with the hypothesis that PMd is mainly involved in managing the task variables related to motor preparation, while DLPFC activity appears more dependent on abstract variables, such as task difficulty (Yamagata et al., 2012).

However, when performing this last analysis, we needed to consider the different RTs between the three monkeys. This control led us to obtain two separate estimates of the target position encoding time in the DLPFC and PMd, one performed by using the brain activity of the same monkey and the other on the brain activity recorded from different monkeys. Even though in both cases we detected an earlier encoding of target position in DLPFC than in PMd, we observed a larger difference in the time lag in the estimate relaying on the sessions coming from two different monkeys (74.3 ms vs 214.7 ms), likely due to the individual differences. To obtain a reliable estimation of the target selection time of the two brain areas, a simultaneous recording from both the DLPFC and PMd would be preferred. A comparable

pattern of neuronal activity in the PFC and PMd evolving with different timings has been observed during the execution of tasks requiring the encoding of abstract rules in matching to sample or quantity comparison tasks (Wallis and Miller, 2003; Vallentin et al., 2012), goal selection in conditional visuomotor tasks (Yamagata et al., 2012) or visual categorization tasks (Cromer et al., 2011). In all these tasks, the PMd cortex was observed to use the task variables to form a motor plan during the time of movement onset and poorly engaged in the encoding task variable not linked to a motor decision (Cromer et al., 2011; Vallentin et al., 2012; Yamagata et al., 2012).

In contrast, the DLPFC is a higher-order brain area involved in encoding abstract variables of decision, such as decision rules (Kim and Shadlen, 1999; Bongard and Nieder, 2010), strategy (Genovesio et al., 2006), behavioral goals (Yamagata et al., 2012; Falcone et al., 2016) or the rank order representation of related information (Brunamonti et al., 2016). There is agreement that the DLPFC sends top-down information to downstream motor areas, such as the PMd, to convert the processing of these variables into motor decision commands (Barbas and Pandya, 1987, 1989; Luppino et al., 2003). According to this model, the involvement of the DLPFC in decision making should occur earlier than the PMd.

However, an earlier involvement of the PMd compared to the DLPFC in encoding the characteristics of the task has also been found (Wallis and Miller, 2003; Cromer et al., 2011). These authors ascribe this early involvement to the familiarity of the monkeys with the task demands and stimuli, which would allow solving the task without the need for an abstract manipulation of the information, a competence supported by PFC (Muhammad et al., 2006). Our experimental protocol hinders such an eventuality. For instance, the monkeys were required to learn the ranked series from a set of never-experienced items randomly selected at the beginning of each experimental session. Thus, this protocol aimed to prevent familiarity with the task stimuli and increase the involvement of the PFC in driving the decision-making-related activity of PMd. In contrast to the discussed results (Wallis and Miller, 2003; Muhammad et al., 2006; Cromer et al., 2011), the time course of the decision-making-related activity of the PFC and PMd observed here fits more with the proposed anatomo-functional model of the relationship between the two brain areas (Barbas and Pandya, 1987, 1989; Luppino et al., 2003)

A further possible role played by the PFC is the orientation of spatial attention (Lennert and Martinez-Trujillo, 2011; Messinger et al., 2021) before the formation of the proper motor plan. Symbolic distance has been observed to modulate the time and magnitude of target selection-related neuronal activity by decreasing the intensity of the neuronal response when the distracting item is easily distinguishable from the target (Lennert and Martinez-Trujillo, 2011). In our data, we observed such modulation of neuronal activity in the DLPFC only in a minority proportion of neurons (14.8%), suggesting that attentional allocation would also act with a different mechanism.

Our results are in accordance with several lines of research on perceptual decision-making in monkeys, converging on the hypothesis that the resolution of the ambiguity of perceptual stimuli supports the selection between competitive motor actions simultaneously available (Cisek and Kalaska, 2005, 2010;

Klaes et al., 2011; Kubanek et al., 2013; Shushruth et al., 2018). Enacting this process, higher-order association areas continuously support the motor system on this decisional computation (Pezzulo and Cisek, 2016; Shushruth et al., 2018). Here, we show that this mechanism can be valid even when ambiguity relates to the representation of information stored in memory.

In summary, the present results support the hypothesis of a hierarchal organization between brain areas in which the DLPFC encodes the variables for decision processes and PMd uses this information to transform abstract decisions in motor programs.

Study 2: Neuronal encoding of ranked items in primate prefrontal cortex during different phases of a transitive inference task

Abstract

Provided with the knowledge that A > B and B > C, individuals are able to infer that A > C. This ability to link the partially overlapping information and extend it to deduce a novel relationship is the basis of a Transitive Inference (TI) capability. Previous neurophysiological studies have described the pattern of neuronal activity from the Prefrontal Cortex being modulated while an abstract mental schema of ranked items is accessed during the inferential reasoning test phase. However, the question of how the neuronal encoding of the rank of individual items subtending this representation is shaped by the learning items' reciprocal relationships is relatively unexplored since very few behavioral neurophysiology studies on animal models are available. In this study, we aimed to answer this question by investigating the single-neuron activity recorded from the dorsolateral prefrontal cortex of two monkeys that learned the rank-ordered series of items as (A>B>C>D>E>F) for solving TI problems. Each session was organized around two consequential Learning phases (learning and consolidation phase), where the relationship between the adjacent items (e.g., A>B, B>C) of the series were first learned separately and then consolidated by presenting them in an intermingled order. Finally, the same pairs, along with the inferential pairs, were presented in the test phase. In each of the experimental sessions, we first searched for a signature of the acquisition of the mental schema in the monkey's performance during Inference. This was behaviorally assessed by observing a symbolic distance effect in each session, which characterizes the comparisons between items with greater rank differences as easier than the ones with smaller rank differences, subtending a comparison between their positions on the mental schema. Then, we studied the single-cell neuronal activity recorded from DLPFC in these sessions while the monkeys fixated each item of the series to define a tuning curve of activity of these neurons during the Test Phase. The tuning activity from the same neurons was then studied during the two previous phases of learning of the task to explore if and how the acquisition of the items' rank order modified the neuron's response. Our results emphasize the involvement of PFC neurons in the learning phases of the TI task by reorganization of rank-ordered activity.

3.1 Introduction

Problem-solving based on deduction is one of the aspects of decision-making widely studied in humans and other species. The ability to make a decision on the basis of manipulation and reorganization of previously acquired knowledge or experiences is termed as reasoning, exhibited by highly encephalized species (Bryant and Trabasso, 1971; McGonigle and Chalmers, 1977; Acuna et al., 2002b). If A>B and B> C, then it can be inferred that A>C. This form of reasoning, when the information is internally manipulated to infer the solution to a novel problem, is called Transitive Inference (TI). TI task is an extensively employed paradigm to study inferential reasoning in humans and non-human animals on mental and neural level (Bryant and Trabasso, 1971; McGonigle and Chalmers, 1977; Dusek and Eichenbaum, 1997; Lazareva and Wasserman, 2006; Brunamonti et al., 2011, 2016; Merritt and Terrace, 2011; Mione et al., 2020). During a TI experiment, the subject is required to learn the preferences between two item pairs presented in a ranked order (A>B, B>C, C>D, D>E, E>F), with each presented pair containing one overlapping item with the previous pair. This learning inherently implies a ranked order A>B>C>D>E>F. Followed to the learning, the subjects are tested for the pairs which have never been presented to them (e.g., B-E), and they are required to make a choice for the higher ranking item by accessing the schema constructed previously. This process accounts for inferential reasoning in such tasks (Acuna et al., 2002b; Brunamonti et al., 2011; Gazes et al., 2012).

A transitive inference task requires the subject to learn, memorize, encode, retrieve and manipulate the information to be able to make inference-based decisions throughout the experiment. Behaviorally, the encoding of the learned information in the form of a mental schema during a TI task is demonstrated through two main effects, the Symbolic distance effect (SDE) and the Serial position effect (SPE) (Acuna et al., 2002b; Merritt and Terrace, 2011; Gazes et al., 2012; Falcone et al., 2016). The SDE refers to the linear increase in performance as the rank difference between the compared items increases (e.g., the comparison between B vs E yields a higher performance as compared to B vs C), while the SPE is a significant decrease in performance as the test pairs (both learned and novel) include the middle items from the ranked series (e.g. the comparisons A vs B and E vs F elicit a higher performance as compared to C vs D).

A vast number of studies have reported how this type of relational memory organization and logical reasoning is supported by a complex hippocampal-cortical network (Acuna et al., 2002a; Kumaran and Maguire, 2006; Zeithamova et al., 2012). Neuroimaging studies in humans have identified the cortical regions activated during tasks involving reasoning and information manipulation during TI (Acuna et al., 2002a; Goel, 2007; Kumaran et al., 2009). Among other cortical regions, these studies have highlighted the role of PFC during the TI task performance attributing it to the executive function of information integration and manipulation in addition to short-term memory (Kumaran et al., 2009). Damage to PFC has been shown to hinder the ability to perform a transitive inference (deductive reasoning; Waltz et al., 1999). In addition to the abundant evidence of major involvement of PFC while

solving a TI task in the aspects of reasoning and manipulation of information by accessing the mental schema, some studies have associated the lateral PFC to sequential and associative learning (Asaad et al., 1998; Reinert et al., 2021). In one of our previous works previous work (Brunamonti et al., 2016), we demonstrated how the activity from dorsolateral PFC (DLPFC) in monkeys is modulated by the behavioral effects (SDE and SPE) during a TI task performance. This study shows that the single-cell activity from DLPFC supports the construction and manipulation of a mental schema of ordered items during the testing phase of the TI task.

However, the question of how this area aids in the acquisition of the information during the learning and how this information is encoded and reorganized from learning to testing during a TI task is still unexplored. To address this question, we recorded and analyzed extracellular activity from the DLPFC of two macaque monkeys while they learned a six-item rank-ordered series (learning phase) and solved the TI problems (test phase). The experimental design of the task is the same used in our previous studies (Brunamonti et al. 2016 and the task schematic for the DLPFC recordings of Sections 2). To study the encoding of the items comprising the ordered series, we studied the tuning activity of the neuronal activity in single cells during each phase and compared this neuronal encoding of items across different phases of the task while the monkeys chose the target item. We also explored if the rank of the series items is encoded by the neuronal population during each task phase and, if so, how it is manipulated from the learning to the test phase.

3.2 Materials and Methods

3.2.1 Subjects

Two male rhesus macaque monkeys (Macaque mulatta), Monkey 1 and Monkey 2, weighing 5.50 kg and 6.50 kg respectively, were trained to learn and perform the TI task. The monkeys were surgically implanted with the recording chambers over the left frontal lobe at the stereotaxic coordinates: anterior-32, lateral-19 (Monkey1); anterior-30, lateral- 18 (Monkey 2). Extracellular neural activity (single unit) was recorded from both the monkeys targeting the dorsal portion of Prefrontal cortex (DLPFC) using a five-channel multielectrode system by Thomas Recording.

All the surgical procedures and animal care considerations were the same as reported for the DLPFC recordings for Monkey1 and Monkey 2 in the previous study (Study 1), which were in accordance with European (Directive 210/63/EU) and Italian (DD.LL. 116/92 and 26/14) laws for non-human primate use for scientific research and were approved by the Italian Ministry of Health.

3.2.2 Behavioral and neuronal data recording

To perform the experiment, the monkeys were seated in a primate chair with their heads fixed. The task was administered by presenting the task stimuli on an interactive 17-inch touchscreen (MicroTouch, sampling rate: 200 Hz). The task stimuli and the behavioral responses were controlled using the freeware software package CORTEX (https://nimh.nih.gov). The eye-movements were monitored and

recorded using an infrared eye tracking device (Arrington Research) at a sampling rate of 220 Hz. The eye position signal and the neuronal activity were synchronized to the behavioral events and they were recorded using an RX6 TDT recording system (Tucker-Davis Technologies, Alachua, FL, USA) during each trial at a sampling rate of 24.4 kHz.

In the current study, we analyzed the data from 13 experimental sessions, with 80 neurons recorded across the sessions of different TI task phases.

3.2.3 Task Design

To implement the transitive inference task for this study, six random stimulus images were selected from a database of 80 abstract black and white images (16^o X 16^o visual angle, bitmaps) at the beginning of each session and ordered arbitrarily to construct a ranked series of items. (Brunamonti et al., 2014, 2016; Mione et al., 2020).

The TI task in this study was implemented through three task phases, the learning phases 1 and 2, and the test phase for each experimental session. During the learning phases, the monkeys were required to learn the reciprocal relationship between the pair of items with adjacent ranks from the ranked series, while during the test phase, the monkeys experienced all the possible combinations of paired items from the series (adjacent and non-adjacent) and they were required to solve the problems using transitive inference (Figure 3.1A).

The learning phase 1 was executed using a sequential learning approach, according to which the pairs with adjacent items in the ranked series were presented and trained in a sequential order to a performance criterion of 90% (Figure 3.1A).

Once the monkey achieved the learning criteria, all the previously learned pairs of items were presented in a random order in larger blocks of trials (learning phase 2). This phase of learning is also termed as the consolidation phase, as all the acquired knowledge during the initial learning phase is consolidated to represent the ranked series of the items in the form of a mental schema.

Following the learning phase 2, the test phase started, during which the monkeys were presented with the learned and the novel pairs of items. To solve the novel pairs, the monkeys had to infer the rank of the individual items learned by them during the learning phase (e.g., in the pair CE, it can be inferred that C is the target item as in the learned pair, CD, C is the reinforced item and in the consequent adjacent pair DE, D is the reinforced item). All the pairs were presented in a random order with at least 14 trials for each pair.

The sequence of the behavioral events for each trial was identical during all the three phases, starting with the appearance of a central target (Red circle with 13.5° × 13.5° visual angle) on the screen to which the monkey had to respond by pushing a button close to the chair within 5 seconds. 200 ms after the button was pushed, the pair of items was presented for a variable epoch (referred as delay; Figure

For more details on the experimental and training procedures, refer to Study 1, Section 2.2

3.1B). After the delay was over, the disappearance of the central target indicated the Go signal, and the monkey was required to choose the higher ranking item by touching it and holding it for 300-350 ms on the monitor. The duration of the delay period in each trial varied from 600 to 1200 ms, while it was 0 ms during the learning phases. The eye-movements were monitored and recorded during the whole session.

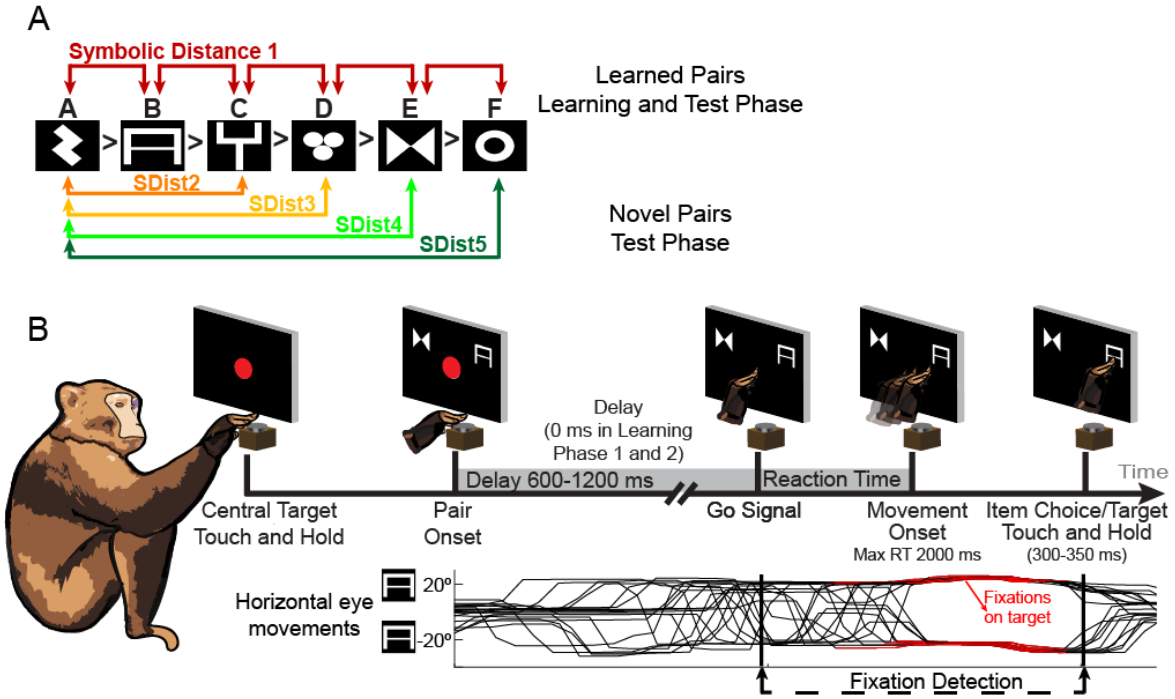

Figure 3.1. Example of an ordered ranked series and the task schematic

A. An example of the ordered series of items and the corresponding Symbolic Distances used for the learning and the test phases of the task. **B)** The schematics of the events during a single trial of the task, followed by the illustration of horizontal eye position signal (bottom plot) for multiple trials during a single session. The eye position signal is represented from the Pair-onset to the target selection, while the fixations on the target (marked in red) were detected between the Go signal and the Item choice. It is to be noted that the eye movements here represent signals from multiple trials, owing to equal probability of the target item to be on the left or the right of the screen (the same item on the two spatial positions represent the probable positions of the target item)

3.2.4 Behavior during test and learning

One of the major behavioral controls during a transitive inference task is the formation of the mental schema at the end of the learning. We tested the presence of this mental schema through the behavior of the animals by testing their performance accuracy and looking for an effect of Symbolic Distance (SDist), defined as the rank difference between the pair items. The Symbolic distance effect explains the formation of a mental schema on the basis of higher probability of picking the correct target, if the distance between the rank of the presented items is higher (i.e. it's easier to identify that B is the correct target item when presented with E as compared to when presented with C). We calculated the percentage of correctly performed trials over total for each SDist.

Following the analysis of behavior in regards with SDist during the test phase, we studied the encoding of each target item comprising the series in the behavior of the subjects throughout the session during the three different phases of the task. To do so, we categorized the trials on the basis of target item during the learning phases and calculated the choice accuracy for each of these subsets of trials. However, during the test phase, we selected the trials characterized only by SDist1 for direct comparison with the trials from learning phases, as only the pairs with adjacent item ranks (SDist1) were presented to the monkey during the learning. Then, we calculated the choice accuracy for each target item for the selected trials of the test phase test phase, and studied if any modulation occurred for the item position in the series.

In addition to the performance accuracy, we analyzed the eye position data for each trial and isolated the time periods when the eye was fixated on one of the target items on the proximity (left or right) of the screen for every session. We identified the fixation duration starting from the target pair onset/go signal to the time when one of the target items was selected by the animal. The target was presented at left (-20̊) or right (+20̊) visual angles in different trials, and we defined a fixation if the eye position signal remained on the target position for at least 100 ms (as illustrated in Figure 3.1B).

3.2.5 Neuronal correlates of rank order during learning and test

Once, we identified the fixation durations during each trial when the animal correctly selected the target item, we analyzed the neuronal activity during these fixation epochs to find a modulation in the neuronal activity from one task phase to another. Subsequently, we studied if the encoding of the items rank was maintained across the three phases of the task. In doing so, we divided the trials based on the target item in the presented pair and selected the epochs from the correct trials when the animal fixated on the correct item to analyze if the neuronal activity evoked by target items characterized by different ordinal ranks differed from each other.

To test if neurons acquired a preference for a specific rank during learning, and if learning modified this preference, we ordered the magnitude of the neuronal activity of neurons from most preferred to the least preferred target item (referred as preferred rank order; Figure 3.3E) during each phase. Followed by this sorting of the neuronal activity according to the rank preference, we fit linear equation $y=ax+c$ to the ordered data and checked if the activity was significantly correlated with the preferred rank order. To see how many neurons were significantly showing a preference for target item ranks, we quantified the number of neurons from each task phase showing a significant linear fitting with the preferred rank order. To test if the rank preference was modified by the learning, we tracked back the neuronal activity according to the ordered data in the test phase and test if a comparable trend was maintained in the two learning phases.

Using this approach, we identified neurons that acquire the preference of a ranked item at the end of learning and neurons that modified it from learning to test.

3.2.6 Decoding analysis

Using a Decoding analysis, we studied differences in the encoding of the item rank across the three different phases of the task on the population level in the studied sample of neurons. To implement this analysis, we used the Neural Decoding Toolbox as described by Meyers, 2013. We calculated the decoding accuracy using the maximum correlation coefficient classifier which makes a mean vector for every class by calculating the average of training data for every class defined for the analysis, and consequently the predictions are made if a test point belongs to a class on the basis of maximum correlation coefficient between the test point and the mean vectors for every class.

To implement this analysis, we analyzed 36 out of 80 neurons, which were recorded from the sessions with at least 5 correct trials for each of the target item correctly selected independently during the learning, consolidation and the test phases. The classifier was trained with the data recorded during the learning, and tested for the consolidation and test phases, and then trained for consolidation and tested for learning and the test phase, and finally trained for test phase and tested for the learning and consolidation phases.

To perform the analysis, we first converted the raster data to the binned format for a bin of 600 ms, starting 600 ms before the target selection. The binned data was therefore characterized by a N-dimensional vector containing the mean spike rate labelled by corresponding conditions for each neuron during the defined bin.

To validate the accuracy of classification process, we randomly selected and grouped the data points equal to the number of splits (k=5; in this case) for each condition from all the available data points for every neuron and created a pseudo-population of neurons. Subsequently, the data was normalized using z-score normalization in order to avoid the differences arising pertaining to the differences in magnitude of the spike rate across the neuronal population. Thereafter, we performed a k-fold cross validation approach, where we used all except one trials for each target rank and task phase were used to train the classifier and the remaining one trial was used for testing the same or the other two task phases. This procedure was repeated the number of time of split using a different test trial in every run. To increase the robustness of the decoding results, the decoding was run 50 times, randomly resampling the trials for training and test splits for the classifier. The decoding accuracy was then averaged over all the runs to calculate the classification accuracy.

To further explore the encoding of the target rank after the learning had been achieved, we repeated the decoding analysis considering two subsets of trials from the test phase, characterized by the SDist1 and the higher symbolic distances. We trained the classifier using the trials from SDist1 from the test phase and then tested the classifier with the subset of trials characterized by SDIst1 and SDist2 to SDist5. This procedure was repeated with the subset of trails from SDist2 to SDist5 as the training set.

3.3 Results

3.3.1 Behavioral performance during the test phase reflects formation of a mental schema

In order to assess if the behavior of the animals during the test phase reflected the formation of a mental schema, we calculated the probability of selecting the correct item as a function of rank differences between the target and the non-target items in the presented pairs (SDist). We observed that the average performance of both the monkeys showed a modulation by the SDist (Figure 3.2A), i.e. the probability of selecting the target item was higher for the higher SDists. This effect was confirmed by a significant correlation between the performance and the SDist ($p<0.01$).

3.3.2 Selection accuracy for different target items is shaped from Learning to Test phase

We calculated the average choice accuracy for the each ranked item in the series, throughout the session and compared them across the different task phases. Figure 3.2B shows the mean performance accuracy when each item was presented as the target with a non-target item. As, observed by the behavior during the learning phase, the choice accuracy for each of the target items is high and does not depend upon the rank of the target item (Figure 3.2B, represented on the x-axis). However, when the session proceeds to the consolidation (learning phase 2), the probability for selecting the target item, when the target item is closer to the extremes of the series is found to be higher as compared to that for the middle items in the series. Subsequently, this reshaping of the choice accuracy for different rank items was prevalent even during the test phase. Here, during the test phase, we analyzed the data only for the SDist1, for a more congruent selection of conditions throughout the task phases. The performance for consolidation in test phases, in Figure 3.2B shows a significant difference across the target items ($ps<0.05$).

Overall, results from the behavioral data analyzed by us are in line with the hypothesis that at the end of the learning procedure the related items are represented on an organized mental schema.

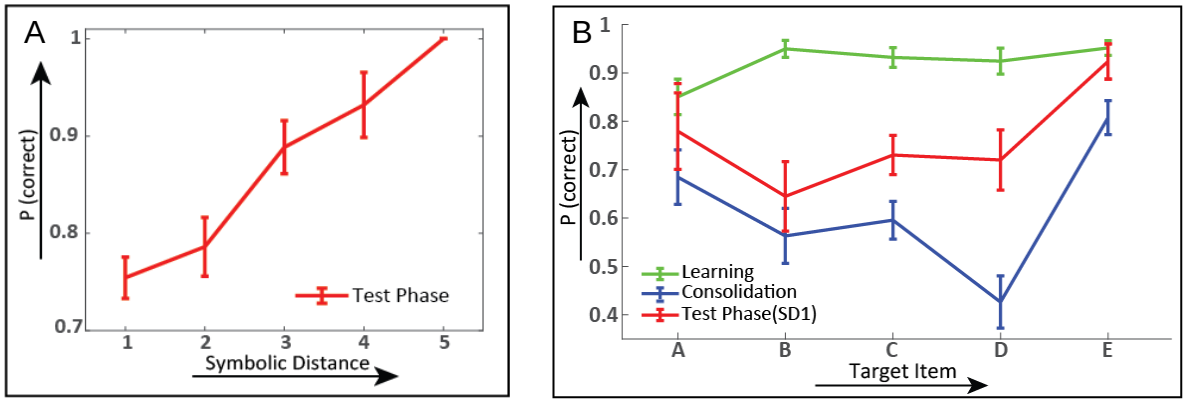

Figure 3.2. Behavioral Correlates of the TI task

A. Mean choice accuracies for both the monkeys (number of sessions=15) during the test phase of the task to select the correct target item as a function of Symbolic Distance. **B.** Mean Choice accuracies for selecting the target item for each pair presentation during Learning Phase, Consolidation Phase and the trials characterized by symbolic distance 1 (SDist1) during the Test Phase.

3.3.3 Encoding and reorganization of neuronal representation of items

Next, we analyzed if items' rank was encoded by the population of studied neurons and how does it change from learning to the test phase of the task. In doing so, we considered the activity from all the neurons in the sample (n=80) across all the three task phases.

Figure 3.3 shows an example neuron of our population of cells exhibiting a significant tuning activity for the ranked list of items only during two phases of the task. Specifically, the neuronal activity is maximal for the item D and decreased for item ranks (Figure 3.3D; test phase). In the other two phases of the task the average activity of the neuron is different from the test phase, even though in consolidation the trend of the tuning activity is comparable to the test phase. To evaluate if the tuning activity was kept across phases, we rank ordered the neuronal activity of the neuron in the test phase, then we used the same order for sorting the neuronal activity during the other two phases (Figure 3.3E, see methods for more details). A linear regression analysis revealed a significant modulation of the ordered activity ($p<0.05$) that was maintained in the consolidation ($p<0.05$) but not in the learning phase ($p>0.05$).

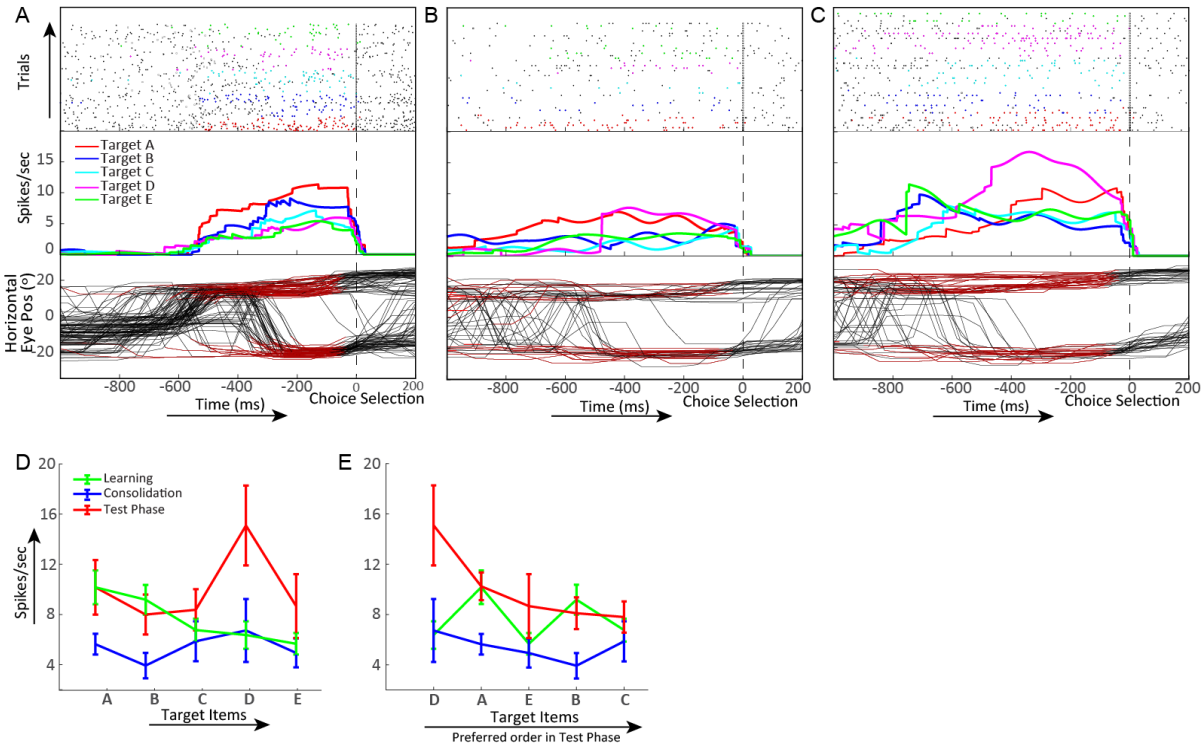

Figure 3.3. Neuronal activity from an example neuron exhibiting an encoding for the item rank during the learning phase. A-C. The top panels show the raster plots for the spikes during each trial, with the activity aligned to the Choice Selection, followed by the spike density function for the mean spike rate corresponding to the trials for each target item during the learning (panel A), the consolidation (panel B) and the test (panel C) phase. The bottom plots show the horizontal eye positions signals, with the fixations on the target item marked in red. **D.** The mean spike rate calculated during the fixation epochs indicated for each trial, plotted as a function of the target item rank. The vertical bars represent SEM, **E.** The rearrangement of the neural activity according to the target rank preferences in test phase.

We repeated this analysis to assess during which phase of the task, the items' rank modulated the neuronal activity and how it changed across the tasks phases. By using this method, we identified different subpopulations of neurons exhibiting an encoding of preferred rank order specifically only during one of the task phases, during two different phases or across all the task phases (Figure 3.4). We found that 75(91.25%) of the total population showed a significant correlation of the neuronal activity with the preferred rank order during at least one of the task phases. Out of this subpopulation, 27 (38.7%), 5 (6.7%) and 12 (16%) cells showed a significant correlation only during the learning phase, the consolidation phase and the test phase respectively. Other group of cells identified by us showed an encoding during two of the task phases, i.e. learning and consolidation, learning and test and lastly the consolidation and test; as represented by the corresponding overlapping areas in the Figure 3.4. And lastly we found that 7(9.3%) cells show a significant encoding of the target rank during each of the task phases (intersection of the three circles in Figure 3.4).

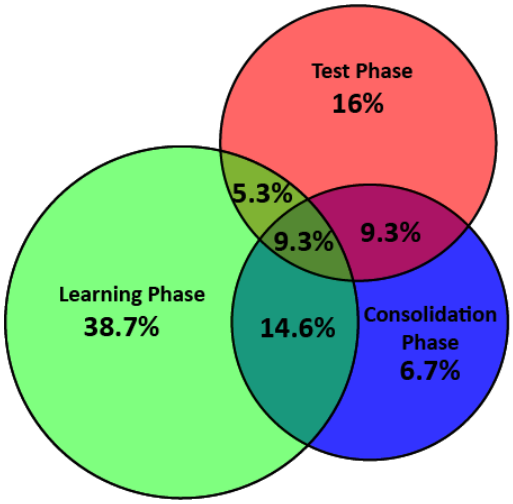

Figure 3.4. Different subpopulations tune for target rank during the TI task phases

The respective percentages of neuronal sub-samples showing a significant linear regression with a preferred rank order during at least one of the task phases.

To further test if the learning of the item relation across the three phases of the task modified the items neuronal encoding we performed a population analysis on three different groups of neurons: 1) neurons displaying a significant linear modulation for the ordered neuronal activity during the learning phase, that was eventually lost in one or both the other phases (n=36; 45 %); 2) neurons displaying a significant linear modulation for the ordered neuronal activity during the test phase, that was eventually lost in one or both the other phases (n=30; 37.5 %); 3) neurons displaying the same encoding of the target ranks across all the three phases (n=9; 11.25%).

Figure 3.5 displays that successive occurrence of the three phases of the task modified the neuronal encoding of the items' set by modifying the initial response tuning of the cells (Figure 3.5A) or by

shaping the response of the neurons at the end of the learning (Figure 3.5 B). Only in a smaller (~11 %) population of neurons did not change the way the items' set modulated the neuronal activity cross the three phases (Figure 3.5 C). Likely this population of neurons kept encoding features of the stimuli that were constant across the task phase as pictorial variables, rather than the items rank order acquired at the end of learning.

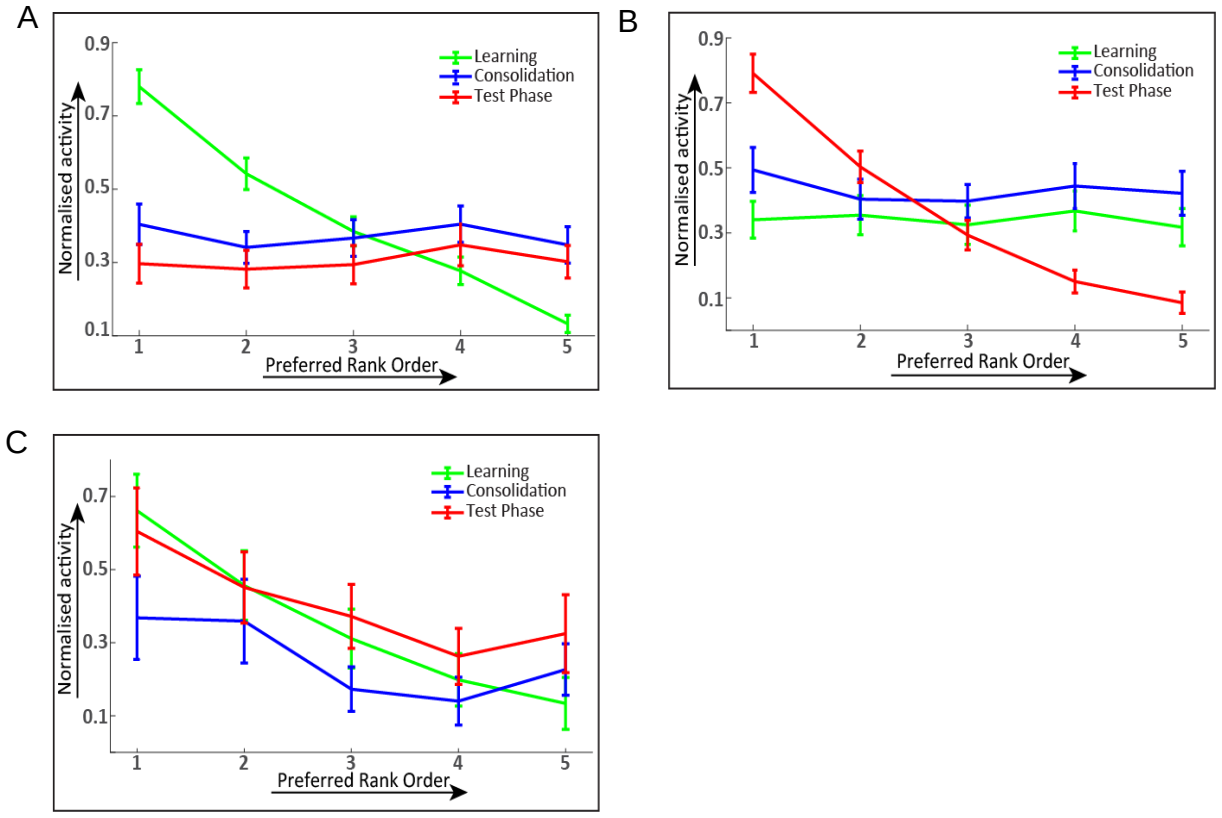

Figure 3.5: Mean spike rate from the subpopulations of cells showing an encoding for the preferred rank order during different task phases.

A. Normalized mean spike rate from the subpopulation encoding the items' rank during the Learning Phase (n=36). The activity of this group of neurons followed a significant linear trend during the learning phase ($p<0.05$) but not in the other phases ($P>0.05$) **B.** during the Test phase (n=30). The activity of this group of neurons followed a significant linear trend during the test phase ($p<0.05$) but not in the other phases ($P>0.05$) and **C.** showing a similar encoding during all the three phases (n=9). The activity of this group of neurons was followed a significant linear trend in all the phases of the task ($p<0.05$); vertical bars represent the SEM.

3.3.4 Neuronal population encodes the target rank differently during different task phases

To have a deeper insight into the differences exhibited by the neurons at a population level while they encode the target rank at different phases of the task from learning of the ranked series to solving the novel problems during the test phase, we performed a decoding analysis using a maximum correlation coefficient classifier (refer to material and methods for further details). This analysis provided us with a classification accuracy calculated on the basis of the spiking patterns for the studied population, to

identify the rank of the target item when the classifier was trained in one of the task phases and tested in the same task phase and the other two task phases. Successively, the classifier was trained for each of the task phases and tested in the similar manner. From the above analysis, we concluded that the classification accuracy is the highest when the classifier is trained and tested in the same block to predict the target item rank. Each plot in the Figure 3.6A shows the average classification accuracy(percentage) when the classifier was trained for one of the task phases and tested with all the three phases of the task (test block: represented on the x-axis). We found that, when the classifier was trained with the learning phase, and tested with consolidation and test phase, the classifier performed significantly above the chance level ($p<0.01$) with the greatest level of accuracy within the same block. The classification accuracy was higher than chance level, when consolidation phase was used as the test block, but still significantly lower ($p<0.001$) than the classification accuracy obtained as a result of training and testing performed within the learning phase. However, when the classifier was tested with the Test phase of the task, the performance of the classifier was close to the chance level and significantly lower than the classification accuracy of within block testing ($p<0.001$). A similar pattern of the performance of the classifier was observed when the classifier was trained with the consolidation phase. Significantly higher classification accuracy was obtained for the testing within the same block when compared with the testing with learning phase ($p<0.001$) and the test phase ($p<0.001$). On the contrary, when the classifier was trained with the test phase, the classification accuracy when tested within the same phase was significantly higher ($p<0.001$) as compared to the performance of the classifier when tested with the learning and consolidation phases. The classifier exhibited a below chance level performance in this case when the training was performed with the test phase and the testing with the two learning phases. Subsequently, using the same population of the neurons, used for the above analysis, we repeated the decoding procedure to compare the spiking activity within the test phase with a different subset of trials from the same task phase. We compared the spiking pattern of the trials from the learned pairs (SDist1) from the learning phase to the trials characterized by the novel pairs during the test phase (SDist 2 to 5). Using this analysis, we observed that once the rank is acquired, the classifier is able to predict the item rank in any condition of the task.

Figure 3.6B shows the plots when the classifier was trained with the trials characterized by SDist1 and tested within the same task conditions (SDist1) and then tested with different task conditions (SDist>1). The classification accuracy obtained by both the testing sets was significantly similar ($p=0.48$). Similar results were found when the classifier was trained with the trials from SDist>1, revealing significantly similar classification accuracies ($p=0.85$). The classifier in all these comparisons was able to efficiently predict the rank of the target item irrespective of the item (non-target) presented alongside, confirmed by the above chance classification accuracies in all the comparisons. The above results indicate that the rank of the target items is encoded by the neuronal population in each of the task phases, however the

same encoding cannot be mapped when looking at the successive phases. Additionally, it suggests, once the learning is achieved, the encoding of the target items is maintained during the test phase of the task.

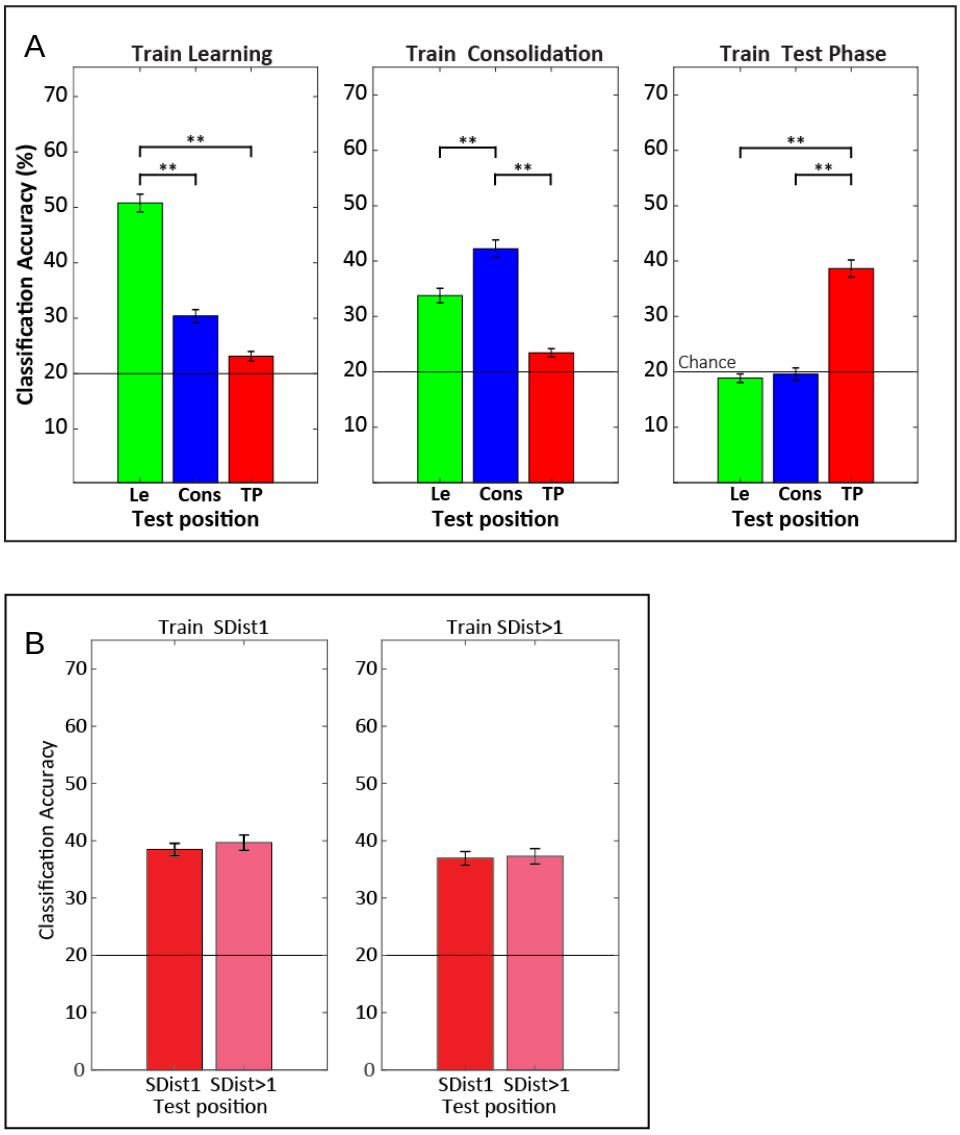

Figure 3.6. Classification accuracies for decoding of the target rank during different task phases

A. The classification accuracies of the classifier for predicting the target item rank when the classifier was trained with the trials from Learning phase (left most plot), Consolidation phase (middle plot) and the Test phase (SDist1; rightmost plot). The x-axis labels represent the test position of the classifier (i.e. Le- Learning, Cons- Consolidation and TP- SDist1 of the Test Phase). The horizontal line represents the chance level and the vertical bars indicate the SEM. **B.** Classification accuracies to identify the target rank calculated as a result of the training and testing the classifier with different task conditions within the Test phase. Learned pairs (SDist1) and the novel pairs (SDist>1).

3.4 Discussion

The learning of new information, encoding it in the memory and inferential reasoning relying on the information indirectly provided during the learning is one of the remarkable cognitive capability of humans and many other species. We studied the neuronal correlates of the encoding of information from learning to testing using an experimental design involving a TI task, where the monkeys had to learn a novel six-item rank ordered series during each session (learning phases) and deduce novel relationships between paired items not experienced previously (test phase). We recorded and analyzed the neuronal activity from the DLPFC of two monkeys while they learned the ordered series and performed choice based decisions by selecting the higher ranking item during a TI task. The results from our study indicate that the DLPFC neurons change the neuronal encoding for the items rank order during the different phases of the task, likely reshaping it in function of the acquired ordinal relation between them.

Previous studies have demonstrated that the monkeys arrange the information in a spatially organized mental schema and it is accessed and manipulated while solving the inferential problems soon after the learning (Merrit and Terrace, 2011; Brunamonti et al 2016; Mione et al 2020). In line with these findings, the behavioral performance from our analysis revealed that the choice accuracy during the test phase of the experiment was directly correlated with the Symbolic Distance, implying the organization of the overlapping relational information as a mental schema.

Furthermore, we observed that the performance related to each target item in the presented pairs was significantly different across the task phases. However, during the learning phase, the performance was not tuned to the rank order of the items. During this phase, each item pair was presented in a sequential order, and the monkey learned the correct target by trial and error which did not necessitate the use of rank order (Acuna et al. 2002b). The learning phase was characterized by the acquiring the relational rules when novel overlapping information was first experienced by the monkeys. However, during the consolidation phase, soon after the hierarchy of the series items was learned by the monkeys, the performance was tuned by the ranked order of the target items i.e. the pairs with extreme series items as target or non-target elicited higher performance than the pairs with middle series items. This effect of Serial position of the target items has been reported by (Merritt and Terrace, 2011), where a SPE has been observed in the performance of the monkeys during the training. However, the effect reported by them is the performance observed during two consecutive training blocks, which by design is similar to the learning and consolidation phases in our task design. We observed a similar tuning of the performance during the test phase, with comparisons between adjacent series items. These results along with the SDE observed during the test phase indicate the formation of a mental schema right after the learning phase.

The role of PFC in solving TI problems and relational reasoning is evident from the previous studies (Waltz et al., 1999; Acuna et al., 2002a; Brunamonti et al., 2016; Spalding et al., 2018). Although there

are very few animal studies which have explored the importance of PFC during the acquisition of the mental schema. (DeVito et al., 2010) have found that a damage to ventro medial PFC hinders the animal's ability to acquire the series of overlapping items (odors in this case) and a major deficit in relation reasoning. These results have shed light on the importance of PFC, not just while performing the transitive problems, but also while forming the mental schema. In our study, we observed that a large proportion of the studied DLPFC neurons encodes the target item ranks even during the learning phase of the task. These results can signal the involvement of DLPFC at this stage of the task in learning new associations in a serial order (Asaad et al., 1998; Kumaran and Maguire, 2006).

By the analysis of DLPFC neuronal activity during the visual attention epochs in the learning phase, the intermediate consolidation phase and the test phase, we found that a huge subpopulation ~92% of the studied sample exhibited a target rank encoding during at least one of the three phases, with only 11% of these neurons exhibited the same target preferences after learning. The majority of the population displays a different encoding of the target rank throughout the task phases. A plausible argument to this observation can be given by the role of these neurons in identifying the individual item (stimulus picture), rather than the relational hierarchy associated with the series items, as reported in a previous study, where the authors have reported a perceptual bias in the dorsal PFC neuronal activity (Wallis and Miller, 2003).

We compared this encoding across the phases while monkeys made a choice from the learned pairs of the items (SDist1). These results are in line with the hypothesis that the overlapping information of the relationships between the adjacent pairs of items is reorganized and manipulated as mental schema is formed and PFC partakes in integration of context based information (Acuna et al., 2002a; Watanabe and Sakagami, 2007; Zeithamova et al., 2012).

The previous studies on TI in animals have reported a modulation of PFC activity with the symbolic distance which is a signature if the task difficulty in this experimental paradigm (Vallentin and Nieder, 2008; Brunamonti et al., 2016). In addition to the modulation by task difficulty during the mental schema retrieval in an inferential reasoning task, PFC has been widely reported to be involved in the short term memory storage (Funahashi, 2006) and encoding of abstract variables during various kinds of decision making like rule encoding (Bongard and Nieder, 2010; La Camera et al., 2018), category learning (Pan et al., 2014), abstract response strategy (Genovesio et al., 2006) and behavioral goals (Yamagata et al., 2012; Falcone et al., 2016). These studies place the PFC in a broader spectrum of learning based functions during a TI task.

The results at a population level also confirm that the target rank is encoded by the DLPFC population across the three different phases, but the way the ranks of the target items are encoded are different for each task phase when looked at the neuronal activity patterns. However, during the test phase, when the target encoding is compared between the learned pairs and the test pairs, no significant differences were observed. These inter-phase differences and similar encoding within the test phase, even when target

items were paired with different non-target items support our hypothesis that the DLPFC activity first supports the construction of the mental schema by aiding to the learning of task rules. Once the information is acquired, it helps in manipulation the information and helps in the construction of a unified mental schema.

Conclusively, these results suggest a role of DLPFC during the learning of the information as the task variables, which has not been explored this form of decision making tasks. Additionally, our results confirm that the DLPFC neurons reshape the activity once the rank order (task rules) is acquired, helping in the organization of the rank ordered information into a mental schema during the inferential reasoning.

Conclusions

In the present work, we investigated the neuronal substrates underlying some of the most complex cognitive mechanisms in the macaque brain. The experimental design used for exploring the effects of deductive reasoning was based on a 6-items series Transitive Inference task. In this thesis, we explored two aspects of neuronal mechanisms underlying inferential reasoning. First, the neuronal correlates of decision-making process leading to the target selection as the constructed mental schema is manipulated. To this aim, we analyzed the single-cell recordings from DLPFC and PMd during the test phase of the task. And second, the neuronal basis of encoding of each series item and the manipulation of mental schema from learning to test phase in DLPFC.

Our results from the first study provide evidence that the DLPFC and PMd, two key areas in decision making, represent the information of the target item in the neuronal activations. However, we found that the DLPFC encodes this information before the PMd, but the activity in PMd, mostly believed to represent more the motor and behavioral response variables, was found to encode the task variable (symbolic distance) during the delay epoch with a comparable degree as the PFC. The representations of target selective activity in PMd modulated by the task difficulty strengthens the hypothesis of the involvement of PMd in more complex cognitive mechanisms. Our findings, along with the findings by Mione et al., 2020, strongly suggest that the PMd plays a major role in decision choice even when the ambiguity in the task performance arises by the representation of the information in memory. Additionally, the involvement of DLPFC in target selectivity before the PMd supports the hypothesis of hierarchical organization of frontal and motor areas, where the decision variables are encoded in DLPFC and then projected onto the PMd, indirectly aiding to motor plan.

The findings from the second study reported in this thesis, however, further explore the involvement of DLPFC in the process of learning and mental schema construction in addition to the previously reported modulation of DLPFC activity during mental schema management (Brunamonti et al., 2016). Our findings highlight the role of DLPFC in the process of acquisition of mental schema during the premise learning in a TI task. These findings are novel in the sense of neurophysiology, as most of the neurophysiological research has explored the involvement of PFC during inferential reasoning. Based on the reported literature from neuroimaging, lesion studies and mice models, the hippocampal cortical circuits enact the information storage as episodic memory, and further, the information is manipulated to deduce inferential problems. Our results show that the DLLPFC neurons show a preference for the

rank of the single items, even during the learning; however, this preference of the rank order changes from learning to the test phase.

From a neurophysiological point of view, these results help us get a step closer to understanding the intricate connections between different brain areas and understanding the functionality of one of the major cognitive control centers of the brain, i.e., DLPFC. The framework involving macaques provides an excellent model for studying the cognitive mechanisms, as their capability to show complex cognitive behaviors, like transitive inference, is comparable to humans. The analysis of the single neuron activity enables a deeper understanding to study area-specific brain functions, as the neuron is the smallest functional unit in the brain, hence providing a very high spatial and temporal resolution. Albeit, there are some considerations that could increase the scope of the results obtained from the above experiments, like the simultaneous acquisition of the neuronal activity from different brain areas. This would provide for a much better temporal comparison across different areas. The scope of these studies can be extended to various directions. The associative learning during the training in TI can be studied in other brain areas (like the motor and visual areas). The analysis of hippocampal activity during a TI task in non-human primates is another promising approach to attain a better understanding of mental schema acquisition. Another notable domain to explore is the task design itself. For example, the implementation of a longer rank-ordered series can augment the chances to study truly transitive test pairs, which are often argued to be non-transitive in nature.

Appendix: Supplementary Information (Study 1)

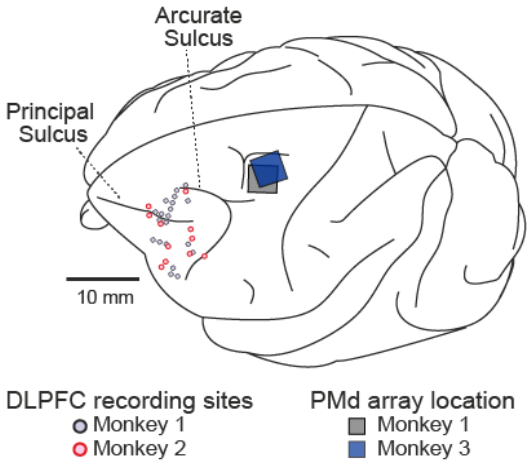

Figure S1: **Recording locations**

Recording sites and array location during DLPFC (Monkey 1 and Monkey 2) and PMd (Monkey 1 and Monkey 3) experiments.

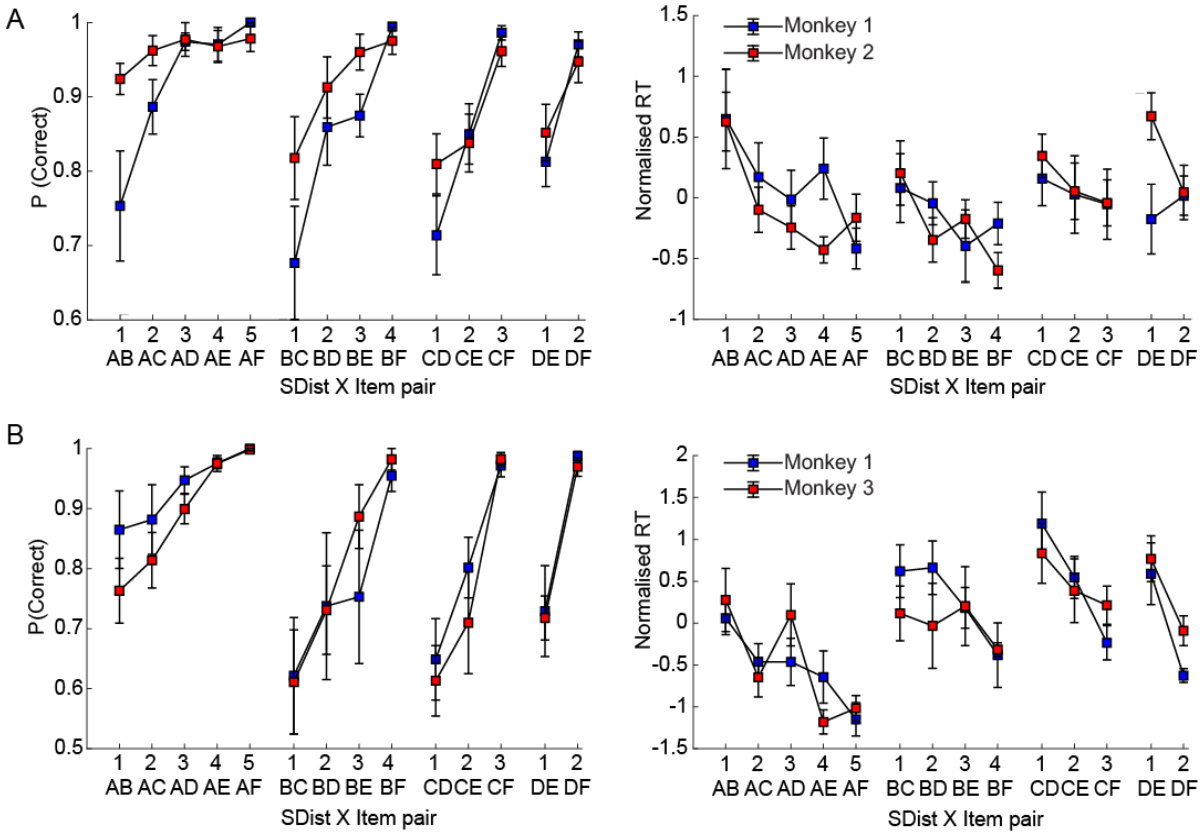

Figure S2: Performance and normalized reaction times for each paired comparison at different symbolic distances: The performance and RTs in selecting the correct target during **A)** DLPFC (Monkey 1: n=14; Monkey 2: n=12) and **B)** PMd (Monkey 1: n=7; Monkey 3: n=7) sessions are represented for each pair organized according

to the symbolic distance characterizing each pair. The vertical bars represent the standard error of mean across the sessions. The proportion of correct choices and the normalized RT for each target item was significantly correlated by the symbolic distance from the presented non-target item (linear regression analysis, all $p<0.05$), except for the RTs of Monkey 1 DLPFC recordings in comparison of item D; and RTs for comparisons of items B and C in the PMd recordings from Monkey 3 ($p>0.05$). The emergence of symbolic distance effect on the performance and RTs for individual items, especially in the case of the item A, which was always rewarded, supports the hypothesis of a mental representation of the ranked items.

Mean abs (D_n)	SDist1	SDist2	SDist3	SDist4	SDist5	Linear Regression Coefficients and statistics
DLPFC						
Delay Epoch (5%)	0.78	0.90	1.08	1.16	1.19	D_n=0.10(SDist)+0.70;p<0.001
RT Epoch (5%)	0.87	0.89	1.08	1.15	1.04	D_n=0.05(SDist)+0.83; p<0.001
Delay Epoch (20%)	1.36	1.36	1.52	1.56	1.54	D_n=0.05(SDist)+1.13; p<0.01
RT Epoch (20%)	1.39	1.43	1.55	1.66	1.68	D_n=0.08(SDist)+1.30; p<0.001
PMd						
Delay Epoch (5%)	0.84	0.96	1.00	1.01	1.31	D_n=0.09(SDist)+0.73; p<0.001
RT Epoch (5%)	1.08	1.01	1.09	1.10	1.19	D_n=0.02(SDist)+1.05; p=0.08
Delay Epoch (20%)	1.13	1.47	1.57	1.52	1.63	D_n=0.05(SDist)+1.37; p<0.001
RT Epoch (20%)	1.40	1.36	1.39	1.43	1.46	D_n=0.01(SDist)+1.35; p=0.06

Table S1: Spatial selectivity (mean abs D_n) for DLPFC and PMd neurons at different selection thresholds and their correlation with SDist.

The evaluation of effect of task difficulty on target position selectivity with different selection criteria of (D_n>5%) and (D_n>20%) revealed higher (DLPFC: 97.1% and PMd:97.2%) and lower (DLPFC: 64% and PMd: 84%) percentages of target selective neurons respectively, when compared to the target position selective population obtained using a criterion of (D_n>10%; DLPFC: 89.3% and PMd: 91.9%). Table S1 reports the mean absolute values of D_n, showing the strength of overall target position selectivity at each SDist. A linear regression analysis revealed that the strength of target position selectivity is significantly correlated with the task difficulty during both the analysis epochs in DLPFC neurons but only during the delay epoch in the PMd neurons even with these selection criteria. Overall these results confirm that at a population level SDist influences the spatial selectivity and that this effect can be detected even applying different criterions of selection of populations of neurons.

Bibliography

Acuna BD, Eliassen JC, Donoghue JP, Sanes JN (2002a) Frontal and parietal lobe activation during transitive inference in humans. Cereb Cortex 12:1312–1321.

Acuna BD, Sanes JN, Donoghue JP (2002b) Cognitive mechanisms of transitive inference. Exp Brain Res 146:1–10.

Asaad WF, Rainer G, Miller EK (1998) Neural Activity in the Primate Prefrontal Cortex during Associative Learning. Neuron 21:1399–1407.

Astrand E, Wardak C, Ben Hamed S (2020) Neuronal population correlates of target selection and distractor filtering. Neuroimage 209:116517.

Barbas H, Pandya DN (1987) Architecture and frontal cortical connections of the premotor cortex (area 6) in the rhesus monkey. J Comp Neurol 256:211–228.

Barbas H, Pandya DN (1989) Architecture and intrinsic connections of the prefrontal cortex in the rhesus monkey. J Comp Neurol 286:353–375.

Basile BM, Templer VL, Gazes RP, Hampton RR (2020) Preserved visual memory and relational cognition performance in monkeys with selective hippocampal lesions. Sci Adv 6.

Benard J, Giurfa M (2004) A Test of Transitive Inferences in Free-Flying Honeybees: Unsuccessful Performance Due to Memory Constraints. Learn Mem 11:328–336.

Bongard S, Nieder A (2010) Basic mathematical rules are encoded by primate prefrontal cortex neurons. Proc Natl Acad Sci 107:2277–2282.

Boussaoud D, Jouffrais C, Bremmer F (1998) Eye position effects on the neuronal activity of dorsal premotor cortex in the macaque monkey. J Neurophysiol 80:1132–1150.

Boysen ST, Berntson GG, Shreyer TA, Quigley KS (1993) Processing of ordinality and transitivity by chimpanzees (Pan troglodytes). J Comp Psychol 107:208–215.

Brunamonti E, Genovesio A, Carbè K, Ferraina S (2011) Gaze modulates non-propositional reasoning: Further evidence for spatial representation of reasoning premises. Neuroscience 173:110–115.

Brunamonti E, Mione V, Di Bello F, De Luna P, Genovesio A, Ferraina S (2014) The NMDAr antagonist ketamine interferes with manipulation of information for transitive inference reasoning in non-human primates. J Psychopharmacol 28:881–887.

Brunamonti E, Mione V, Di Bello F, Pani P, Genovesio A, Ferraina S (2016) Neuronal Modulation in the Prefrontal Cortex in a Transitive Inference Task: Evidence of Neuronal Correlates of Mental

Schema Management. J Neurosci 36:1223–1236.

Bryant PE, Trabasso T (1971) Transitive Inferences and Memory in Young Children. Nature 232:456–458.

Burt C (1911) Experimental tests of higher mental processes and their relation to general intelligence. J Exp Pedagog Train 1:93–112.

Burt C (2011) The development of reasoning in children. In: Experimental psychology and child study., pp 53–63 The new educators library. London, Great Britain: Sir Isaac Pitman & Sons.

Caminiti R, Ferraina S, Mayer AB (1998) Visuomotor transformations: Early cortical mechanisms of reaching. Curr Opin Neurobiol 8:753–761.

Caminiti R, Johnson P, Galli C, Ferraina S, Burnod Y (1991) Making arm movements within different parts of space: the premotor and motor cortical representation of a coordinate system for reaching to visual targets. J Neurosci 11:1182–1197.

Carlson S, Rämä P, Tanila H, Linnankoski I, Mansikka H (1997) Dissociation of Mnemonic Coding and Other Functional Neuronal Processing in the Monkey Prefrontal Cortex. J Neurophysiol 77:761–774.

Chandrasekaran C, Peixoto D, Newsome WT, Shenoy K V. (2017) Laminar differences in decision-related neural activity in dorsal premotor cortex. Nat Commun 8.

Churchland MM (2006) Neural Variability in Premotor Cortex Provides a Signature of Motor Preparation. J Neurosci 26:3697–3712.

Cisek P, Kalaska JF (2005) Neural Correlates of Reaching Decisions in Dorsal Premotor Cortex: Specification of Multiple Direction Choices and Final Selection of Action. Neuron 45:801–814.

Cisek P, Kalaska JF (2010) Neural Mechanisms for Interacting with a World Full of Action Choices. Annu Rev Neurosci 33:269–298.

Coallier É, Kalaska JF (2014) Reach target selection in humans using ambiguous decision cues containing variable amounts of conflicting sensory evidence supporting each target choice. J Neurophysiol 112:2916–2938.

Coallier É, Michelet T, Kalaska JF (2015) Dorsal premotor cortex: neural correlates of reach target decisions based on a color-location matching rule and conflicting sensory evidence. J Neurophysiol 113:3543–3573.

Constantinescu AO, O'Reilly JX, Behrens TEJ (2016) Organizing conceptual knowledge in humans with a gridlike code. Science (80-) 352:1464–1468.

Cromer JA, Roy JE, Buschman TJ, Miller EK (2011) Comparison of Primate Prefrontal and Premotor

Cortex Neuronal Activity during Visual Categorization. J Cogn Neurosci 23:3355–3365.

D'Amato MR, Colombo M (1990) The symbolic distance effect in monkeys (Cebus apella). Anim Learn Behav 18:133–140.

Daisley JN, Vallortigara G, Regolin L (2021) Low-rank Gallus gallus domesticus chicks are better at transitive inference reasoning. Commun Biol 4:1344.

DeVito LM, Lykken C, Kanter BR, Eichenbaum H (2010) Prefrontal cortex: Role in acquisition of overlapping associations and transitive inference. Learn Mem 17:161–167.

Diester I, Nieder A (2007) Semantic Associations between Signs and Numerical Categories in the Prefrontal Cortex Dehaene S, ed. PLoS Biol 5:e294.

Donahue CH, Lee D (2015) Dynamic routing of task-relevant signals for decision making in dorsolateral prefrontal cortex. Nat Neurosci 18:295–301.

Dusek JA, Eichenbaum H (1997) The hippocampus and memory for orderly stimulus relations. Proc Natl Acad Sci 94:7109–7114.

Falcone R, Brunamonti E, Ferraina S, Genovesio A (2016) Neural Encoding of Self and Another Agent's Goal in the Primate Prefrontal Cortex: Human–Monkey Interactions. Cereb Cortex 26:4613–4622.

Ferraina S, Battaglia-Mayer A, Genovesio A, Marconi B, Onorati P, Caminiti R (2001) Early Coding of Visuomanual Coordination During Reaching in Parietal Area PEc. J Neurophysiol 85:462–467.

Fine JM, Hayden BY (2022) The whole prefrontal cortex is premotor cortex. Philos Trans R Soc B Biol Sci 377:1–32.

Freedman DJ (2001) 2001, Freedman et al - Categorical Representation of. 291.

Funahashi S (2001) Neuronal mechanisms of executive control by the prefrontal cortex. Neurosci Res 39:147–165.

Funahashi S (2006) Prefrontal cortex and working memory processes. Neuroscience 139:251–261.

Funahashi S, Bruce CJ, Goldman-Rakic PS (1989) Mnemonic coding of visual space in the monkey's dorsolateral prefrontal cortex. J Neurophysiol 61:331–349.

Fusi S, Miller EK, Rigotti M (2016) Why neurons mix: high dimensionality for higher cognition. Curr Opin Neurobiol 37:66–74.

Gazes RP, Chee NW, Hampton RR (2012) Cognitive mechanisms for transitive inference performance in rhesus monkeys: Measuring the influence of associative strength and inferred

order. J Exp Psychol Anim Behav Process 38:331–345.

Genovesio A, Brasted PJ, Wise SP (2006) Representation of Future and Previous Spatial Goals by Separate Neural Populations in Prefrontal Cortex. J Neurosci 26:7305–7316.

Gillan DJ, Premack D, Woodruff G (1981) Reasoning in the Chimpanzee. J Exp Psychol 7:1–17.

Goel V (2004) Differential involvement of left prefrontal cortexin inductive and deductive reasoning. Cognition 93:B109–B121.

Goel V (2007) Anatomy of deductive reasoning. Trends Cogn Sci 11:435–441.

Goel V, Buchel C, Frith C, Dolan RJ (2000) Dissociation of Mechanisms Underlying Syllogistic Reasoning. Neuroimage 12:504–514.

Goel V, Dolan RJ (2001) Functional neuroanatomy of three-term relational reasoning. Neuropsychologia 39:901–909.

Gold JI, Shadlen MN (2007) The Neural Basis of Decision Making. Annu Rev Neurosci 30:535–574.

Goldman-Rakic PS (1988) Topography of Cognition: Parallel Distributed Networks in Primate Association Cortex. Annu Rev Neurosci 11:137–156.

Grafton ST, Volz LJ (2019) From ideas to action: The prefrontal–premotor connections that shape motor behavior. In: Handbook of Clinical Neurology (D'Esposito M, Grafman JHBT-H of CN, eds), pp 237–255. Elsevier.

Grosenick L, Clement TS, Fernald RD (2007) Erratum: Fish can infer social rank by observation alone. Nature 446:102–102.

Heckers S, Zalesak M, Weiss AP, Ditman T, Titone D (2004) Hippocampal activation during transitive inference in humans. Hippocampus 14:153–162.

Hoshi E, Tanji J (2000) Integration of target and body-part information in the premotor cortex when planning action. Nature 408:466–470.

Iba M, Sawaguchi T (2002) Neuronal activity representing visuospatial mnemonic processes associated with target selection in the monkey dorsolateral prefrontal cortex. Neurosci Res 43:9–22.

Jensen G (2017) Serial learning. In: APA handbook of comparative psychology: Perception, learning, and cognition., pp 385–409 APA handbooks in psychology®. Washington: American Psychological Association.

Jensen G, Ferrera VP, Terrace HS (2021) Positional inference in rhesus macaques. Anim Cogn.

Jensen G, Terrace HS, Ferrera VP (2019) Discovering Implied Serial Order Through Model-Free and

Model-Based Learning. Front Neurosci 13:1–24.

Johnson PB, Ferraina S, Bianchi L, Caminiti R (1996) Cortical networks for visual reaching: Physiological and anatomical organization of frontal and parietal lobe arm regions. Cereb Cortex 6:102–119.

Kim J-N, Shadlen MN (1999) Neural correlates of a decision in the dorsolateral prefrontal cortex of the macaque. Nat Neurosci 2:176–185.

Klaes C, Westendorff S, Chakrabarti S, Gail A (2011) Choosing Goals, Not Rules: Deciding among Rule-Based Action Plans. Neuron 70:536–548.

Knauff M, Fangmeier T, Ruff CC, Johnson-Laird PN (2003) Reasoning, Models, and Images: Behavioral Measures and Cortical Activity. J Cogn Neurosci 15:559–573.

Kubanek J, Wang C, Snyder LH (2013) Neuronal responses to target onset in oculomotor and somatomotor parietal circuits differ markedly in a choice task. J Neurophysiol 110:2247–2256.

Kumaran D, Maguire EA (2006) The dynamics of hippocampal activation during encoding of overlapping sequences. Neuron 49:617–629.

Kumaran D, Summerfield JJ, Hassabis D, Maguire EA (2009) Tracking the Emergence of Conceptual Knowledge during Human Decision Making. Neuron 63:889–901.

Kurata K, Hoffman DS (1994) Differential effects of muscimol microinjection into dorsal and ventral aspects of the premotor cortex of monkeys. J Neurophysiol 71:1151–1164.

Kurata K, Wise SP (1988) Premotor cortex of rhesus monkeys: set-related activity during two conditional motor tasks. Exp Brain Res 69:327–343.

La Camera G, Bouret S, Richmond BJ (2018) Contributions of Lateral and Orbital Frontal Regions to Abstract Rule Acquisition and Reversal in Monkeys. Front Neurosci 12:1–17.

Lazareva OF, Paxton Gazes R, Elkins Z, Hampton R (2020) Associative models fail to characterize transitive inference performance in rhesus monkeys (Macaca mulatta). Learn Behav 48:135–148.

Lazareva OF, Smirnova AA, Bagozkaja MS, Zorina ZA, Rayevsky V V., Wasserman EA (2004) TRANSITIVE RESPONDING IN HOODED CROWS REQUIRES LINEARLY ORDERED STIMULI. J Exp Anal Behav 82:1–19.

Lazareva OF, Wasserman EA (2006) Effect of stimulus orderability and reinforcement history on transitive responding in pigeons. Behav Processes 72:161–172.

Lebedev MA, Wise SP (2001) Tuning for the orientation of spatial attention in dorsal premotor cortex. Eur J Neurosci 13:1002–1008.

Lennert T, Martinez-Trujillo J (2011) Strength of Response Suppression to Distracter Stimuli Determines Attentional-Filtering Performance in Primate Prefrontal Neurons. Neuron 70:141–152.

Lennert T, Martinez-Trujillo JC (2013) Prefrontal Neurons of Opposite Spatial Preference Display Distinct Target Selection Dynamics. J Neurosci 33:9520–9529.

Luppino G, Rozzi S, Calzavara R, Matelli M (2003) Prefrontal and agranular cingulate projections to the dorsal premotor areas F2 and F7 in the macaque monkey. Eur J Neurosci 17:559–578.

McGonigle BO, Chalmers M (1977) Are monkeys logical? Nature 267:694–696.

Merritt DJ, Terrace HS (2011) Mechanisms of inferential order judgments in humans (Homo sapiens) and rhesus monkeys (Macaca mulatta). J Comp Psychol 125:227–238.

Messinger A, Cirillo R, Wise SP, Genovesio A (2021) Separable neuronal contributions to covertly attended locations and movement goals in macaque frontal cortex. Sci Adv 7:1–15.

Meyers EM (2013) The neural decoding toolbox. Front Neuroinform 7:8.

Mione V, Brunamonti E, Pani P, Genovesio A, Ferraina S (2020) Dorsal Premotor Cortex Neurons Signal the Level of Choice Difficulty during Logical Decisions. Cell Rep 32:107961.

Muhammad R, Wallis JD, Miller EK (2006) A Comparison of Abstract Rules in the Prefrontal Cortex, Premotor Cortex, Inferior Temporal Cortex, and Striatum. J Cogn Neurosci 18:974–989.

Munoz F, Jensen G, Kennedy BC, Alkan Y, Terrace HS, Ferrera VP (2020) Learned Representation of Implied Serial Order in Posterior Parietal Cortex. Sci Rep 10:9386.

Pan X, Fan H, Sawa K, Tsuda I, Tsukada M, Sakagami M (2014) Reward Inference by Primate Prefrontal and Striatal Neurons. J Neurosci 34:1380–1396.

Pan X, Sawa K, Tsuda I, Tsukada M, Sakagami M (2008) Reward prediction based on stimulus categorization in primate lateral prefrontal cortex. Nat Neurosci 11:703–712.

Paz-y-Miño C G, Bond AB, Kamil AC, Balda RP (2004) Pinyon jays use transitive inference to predict social dominance. Nature 430:778–781.

Pezzulo G, Cisek P (2016) Navigating the Affordance Landscape: Feedback Control as a Process Model of Behavior and Cognition. Trends Cogn Sci 20:414–424.

Piaget J (1930) Judgment and Reasoning in the Child. NY, Harcourt Brace and Co., 1928, 260 pp. Child's Concept Phys Causality NY, Harcourt Brace Co.

Piaget J (1955) The child's construction of reality. Routledge & Kegan Paul.

Piaget J (1970) Science of education and the psychology of the child. Trans. D. Coltman.

Reinert S, Hübener M, Bonhoeffer T, Goltstein PM (2021) Mouse prefrontal cortex represents learned rules for categorization. Nature 593:411–417.

Sheahan H, Luyckx F, Nelli S, Teupe C, Summerfield C (2021) Neural state space alignment for magnitude generalization in humans and recurrent networks. Neuron 109:1214-1226.e8.

Shushruth S, Mazurek M, Shadlen MN (2018) Comparison of Decision-Related Signals in Sensory and Motor Preparatory Responses of Neurons in Area LIP. J Neurosci 38:6350–6365.

Spalding KN, Schlichting ML, Zeithamova D, Preston AR, Tranel D, Duff MC, Warren DE (2018) Ventromedial Prefrontal Cortex Is Necessary for Normal Associative Inference and Memory Integration. J Neurosci 38:3767–3775.

Sternberg RJ (1980) Representation and process in linear syllogistic reasoning. J Exp Psychol Gen 109:119–159.

Stuss DT, Benson DF (1986) The Frontal Lobes. Raven Press.

Thompson, Kirk G., Doug P. Hanes, Narcisse P. Bichot, and Jeffrey D. Schall. 1996. “Perceptual and Motor Processing Stages Identified in the Activity of Macaque Frontal Eye Field Neurons during Visual Search.” *Journal of Neurophysiology* 76(6): 4040–55.

Trabasso T, Riley CA (1975) The construction and use of representations involving linear order. Inf Process Cogn Loyola Symp:381–410.

Treichler FR, Raghanti MA, Van Tilburg DN (2003) Linking of serially ordered lists by macaque monkeys (Macaca mulatta): List position influences. J Exp Psychol Anim Behav Process 29:211–221.

Treichler FR, Van Tilburg D (1996) Concurrent conditional discrimination tests of transitive inference by macaque monkeys: List linking. J Exp Psychol Anim Behav Process 22:105–117.

Vallentin D, Bongard S, Nieder A (2012) Numerical Rule Coding in the Prefrontal, Premotor, and Posterior Parietal Cortices of Macaques. J Neurosci 32:6621–6630.

Vallentin D, Nieder A (2008) Behavioral and Prefrontal Representation of Spatial Proportions in the Monkey. Curr Biol 18:1420–1425.

Van Elzakker M, O’Reilly RC, Rudy JW (2003) Transitivity, flexibility, conjunctive representations, and the hippocampus. I. An empirical analysis. Hippocampus 13:334–340.

Vasconcelos M (2008) Transitive inference in non-human animals: An empirical and theoretical analysis. Behav Processes 78:313–334.

Von Fersen L, Wynne CDL, Delius JD, Staddon JER (1991) Transitive inference formation in pigeons. J Exp Psychol Anim Behav Process 17:334–341.

Wallis JD, Miller EK (2003) From Rule to Response: Neuronal Processes in the Premotor and Prefrontal Cortex. J Neurophysiol 90:1790–1806.

Waltz JA, Knowlton BJ, Holyoak KJ, Boone KB, Mishkin FS, de Menezes Santos M, Thomas CR, Miller BL (1999) A System for Relational Reasoning in Human Prefrontal Cortex. Psychol Sci 10:119–125.

Watanabe M (1986) Prefrontal unit activity during delayed conditional Go/No-go discrimination in the monkey. II. Relation to Go and No-go responses. Brain Res 382:15–27.

Watanabe M, Sakagami M (2007) Integration of Cognitive and Motivational Context Information in the Primate Prefrontal Cortex. Cereb Cortex 17:i101–i109.

Weaver JE, Steirn JN, Zentall TR (1997) Transitive inference in pigeons: Control for differential value transfer. Psychon Bull Rev 4:113–117.

Weinrich M, Wise S (1982) The premotor cortex of the monkey. J Neurosci 2:1329–1345.

Wise S (1985) The Primate Premotor Cortex: Past, Present, and Preparatory. Annu Rev Neurosci 8:1–19.

Wise SP, Di Pellegrino G, Boussaoud D (1992) Primate premotor cortex: dissociation of visuomotor from sensory signals. J Neurophysiol 68:969–972.

Woocher FD, Glass AL, Holyoak KJ (1978) Positional discriminability in linear orderings. Mem Cognit 6:165–173.

Wynne CDL (1997) Pigeon transitive inference: Tests of simple accounts of a complex performance. Behav Processes 39:95–112.

Yamagata T, Nakayama Y, Tanji J, Hoshi E (2012) Distinct Information Representation and Processing for Goal-Directed Behavior in the Dorsolateral and Ventrolateral Prefrontal Cortex and the Dorsal Premotor Cortex. J Neurosci 32:12934–12949.

Zeithamova D, Dominick AL, Preston AR (2012) Hippocampal and Ventral Medial Prefrontal Activation during Retrieval-Mediated Learning Supports Novel Inference. Neuron 75:168–179.

Zeithamova D, Mack ML, Braunlich K, Davis T, Seger CA, van Kesteren MTR, Wutz A (2019) Brain Mechanisms of Concept Learning. J Neurosci 39:8259–8266.